Distribution of the order parameter in strongly disordered superconductors: An analytic theory

Anton V. Khvalyuk [*]
Skolkovo Institute of Science and Technology, 143026 Skolkovo, Russia
and L. D. Landau Institute for Theoretical Physics, Kosygin Str. 2, Moscow 119334, Russia

Mikhail V. Feigel'man [†]
L. D. Landau Institute for Theoretical Physics, Kosygin Str. 2, Moscow 119334, Russia
and Moscow Institute of Physics and Technology, Dolgoprudny, Moscow 141701, Russia

(Received 3 July 2021; revised 13 November 2021; accepted 23 November 2021; published 15 December 2021)

We developed an analytic theory of inhomogeneous superconducting pairing in strongly disordered materials, which are moderately close to superconducting-insulator transition. Single-electron eigenstates are assumed to be Anderson localized, with a large localization volume. Superconductivity develops due to coherent delocalization of originally localized preformed Cooper pairs. The key assumption of the theory is that each such pair is coupled to a large number $Z \gg 1$ of similar neighboring pairs. We derived integral equations for the probability distribution $P(\Delta)$ of local superconducting order parameter $\Delta(\boldsymbol{r})$ and analyzed their solutions in the limit of small dimensionless Cooper coupling constant $\lambda \ll 1$. The shape of the order-parameter distribution is found to depend crucially upon the effective number of nearest neighbors $Z_{\rm eff} = 2\nu_0\Delta_0 Z$, with ν_0 being the single-particle density of states at the Fermi level. The solution we provide is valid both at large and small $Z_{\rm eff}$; the latter case is nontrivial as the function $P(\Delta)$ is heavily non-Gaussian. One of our key findings is the discovery of a broad range of parameters where the distribution function $P(\Delta)$ is non-Gaussian but also noncritical (in the sense of superconductor-insulator transition criticality). The analytic results are supplemented by numerical data and good agreement between them is observed.

DOI: 10.1103/PhysRevB.104.224505

I. INTRODUCTION

Strongly disordered superconductors are interesting both from fundamental and practical perspectives. The fundamental problem of a quantum (zero-temperature) phase transition between superconducting and insulating ground states [superconductor-insulator transition (SIT)] has attracted considerable attention since the mid-'80s [1–5] and got an additional burst of research during the last decade. Prominent examples include various structurally different realizations of the SIT, such as granular arrays of Josephson junctions or thick homogeneous films of amorphous indium oxide. The whole variety of phenomena collectively labeled as SIT demonstrate a great deal of diversity in the underlying physics and thus cannot be possibly explained by a single mechanism (see a recent review [6] for further details). In this paper, we theoretically demonstrate several rather persistent properties of 3D materials with homogeneous structure and strong microscopic disorder.

The practical side of interest in strongly disordered superconductors stems from potential applications in quantum computing technologies in the form of so-called superinductors [7–11]. These are much wanted yet, so far, mostly hypothetical inductive devices combine nearly absent dissipation at low energies (in GHz range) with high inductance and small spatial size such that kinetic inductance per square $L_\square$ exceeds 10 nH. The principal opportunity to fabricate such a device is provided by the platform of thick films of strongly disordered superconductors. Indeed, the latter feature low superfluid density ρ_s and the associated high kinetic inductance per square $L_\square \sim 1/\rho_s$, enabling one to implement an superinductor within a compact geometry. Such extreme values for these materials are a consequence of high normal state resistance induced by disorder [12, Sec. 3.10][13][14, Figs. 3(b) and 3(c) in particular]. On the other hand, the necessity for the absence of low-energy dissipation requires one to use materials with a well-resolved gap in the optical excitation spectrum—a feature so natural for superconducting materials.

However, it occurs that the two conditions mentioned above (low ρ_s and absence of any low-energy excitations) come into conflict. Superconductors which are *too close to SIT* unavoidably contain some nonzero density of low-lying collective modes even when single-electron density of states (1-DoS) is fully gapped, as demonstrated by theoretical analysis [15] and experimental observations [13]. Yet, the question of low-energy modes in strongly disordered superconductors is by no means resolved qualitatively. The preliminary analysis performed in Ref. [15] was based upon the approximation of constant superconducting order parameter $\Delta(\mathbf{r}) = \Delta$, which is far from being obviously correct. Instead, a self-consistent theory of the system's collective modes without

[*] anton.k@itp.ac.ru
[†] feigel@landau.ac.ru

the use of such a drastic approximation is needed. Moreover, the spatial distribution of superconducting order parameter can now be probed by means of modern low-temperature scanning tunneling microscopy methods [16–20]. It is thus of both fundamental and practical interest to develop a theory that would be able to (1) describe realistic spatial distributions of the order parameter and (2) describe the behavior of collective modes on top of the spatially inhomogeneous superconducting state. In the present paper, we deal with the first of these problems only, leaving the second one for the near future.

The local probability distribution function $P(\Delta)$ of the superconducting order parameter has already been addressed in several important limiting cases of disorder strength. The limit of small disorder corresponds to usual dirty superconductors with diffusive transport in the normal state. For this regime, the structure of statistical fluctuations of the order parameter was analyzed in a seminal paper [21, see Sec. 3, in particular] by means of semiclassical theory of superconductivity, demonstrating a narrow purely Gaussian $P(\Delta)$. In the opposite limit of small disorder, the single-electron wave functions suffer Anderson localization transition, rendering the conventional semiclassical approach inapplicable. To describe this regime, Ref. [22] substantiated the model on the Bethe lattice, while a subsequent paper [23] showed that the resulting $P(\Delta)$ exhibits critical features, such as fat tails extended to the region of large Δ, much larger than the typical value Δ_{typ}. However, realistic experiments usually deal with superconducting samples, which fall within neither of the two limiting cases described above; it is especially so for superconductors which may serve as candidates for construction of superinductors. On the one hand, superconducting materials discussed in the work are *much more disordered* than usual dirty superconductors, to the extent where neither the standard semiclassical theory of Ref. [21] nor even the mere Gaussian approximation for $P(\Delta)$ are applicable. As suggested by numerical data [24,29] and experimental observations [17,20,25], this type of material features heavily non-Gaussian profiles of the order parameter distribution. On the other hand, the level of disorder, the resulting noncritical distribution $P(\Delta)$, and the requirement for the absence of low-energy excitations are all suggesting that the samples of interest are *somewhat away from the SIT*, so the critical theory of Ref. [23] is also inapplicable. The present paper is devoted to the development of analytical methods able to study the order parameter distribution in materials that belong to the region in between the two limiting cases. The latter turns out to be parametrically broad, as we also show below. While our approach is general and valid *in principle* at all temperatures, in this paper we consider $T = 0$ limit only.

This paper is organized as follows. We formulate our theoretical model in Sec. II. Within it, we review the relevant phenomenology of disordered superconductors and formulate the Hamiltonian of the system. The corresponding static self-consistency equations for the order parameter are then introduced along with a brief discussion of applicability and several known limits. The section is closed by a brief discussion of the methods used in previous works to analyze problems similar to the one stated in the present work. Section III then presents the body of our theoretical approach. In Sec. III A, we start by deriving a general set of equations to describe the statistics of solution to systems of local *nonlinear* equations with disorder, such as the self-consistency equations for the order parameter. Within the following Sec. III B, those equations are substantially simplified in the physically relevant limit of small order parameter $\nu_0\Delta_0 \ll 1$ and large number of neighbors $Z \gg 1$ within the localization volume of a given single-particle state. Such simplifications render the presented equations amenable for both numerical and analytical analysis. In Sec. III C, the reader can find an explicit *analytical* solution to the proposed equations on the distribution function of the order parameter and related quantities in terms of certain special functions. The following Sec. III E then briefly describes the numerical routines used to analyze both the original self-consistency equations in a particular realization of disorder in the system and the derived equations on the distributions of various physical quantities across different disorder realizations. In Sec. III F, we demonstrate the key outcomes of our theoretical analysis: The profile of the distribution function as a function of the parameters of the model and the asymptotic behavior of the distribution. The subsection also contains some results for the distribution of other local physical quantities. Section III G then introduces and analyzes several important extensions of our model that allow us to draw conclusions about the robustness of our findings. Finally, Sec. IV summarizes the key theoretical achievements and outlines several immediate developments. This paper is accompanied by the Supplemental Material (SM) [26] that contains additional technical information on various steps of theoretical and numerical analysis employed in this paper.

II. THE MODEL

A. Phenomenology of strongly disordered superconductors

The physics of SIT owes its rich phenomenology to the underlying complexity of the Anderson localization transition in the single-particle spectrum of the system. Reference [27] conducts an extensive research of the topic, building upon a seminal paper [28] and early numerical studies [24]; here we employ a simplified description proposed and substantiated in Refs. [22,23].

The single-particle electron states are described by spatially localized wave functions $\psi_i(r)$ with large localization volume V_{loc} and complex spatial structure [27, Sec. 2]. The single-particle eigenenergies ξ_i of these states can be approximated as randomly distributed independent variables, with the typical width of the distribution $\nu(\xi)$ being of order of the Fermi energy E_F. We assume that this distribution arranges a finite DoS *per spin projection* $\nu_0 = \nu(\xi = 0) \sim 1/E_F$ at the Fermi level.

Even prior to the emergence of the global superconducting coherence, the systems in question are known to favor the formation of localized Cooper pairs [27, Sec. 3 and references therein]. This phenomenon can be delineated by an additional energy E_{PG} per each unpaired electron in the system. For the systems of interest, the typical scale of E_{PG} is significantly larger than all superconducting

energy scales [27, Sec. 4.3]. Consequently, single-particle excitations barely contribute to low-energy physics. One is thus able to describe the relevant physics by considering only the states corresponding to presence or absence of a local Cooper pair on a given single-particle state i, effectively halving the Hilbert space, as described in Ref. [27, Sec. 6].

The superconducting order in the system then corresponds to coherent delocalization of preformed Cooper pairs, as demonstrated experimentally in Ref. [17] and supported by numerical data [29]. Such behavior results from attractive Cooper-like pairwise interaction between the Cooper pairs. This interaction is assumed to be local, so it only connects single-particle states with a finite spatial overlap. As a result, each single-particle state i is effectively interacting with other states located within the localization volume of i. However, the particular subset of those states is rather nontrivial due to both the complex structure of the single-particle wave functions $\psi_i(r)$ and explicit dependence of the matrix element of the interaction on energy difference $\xi_i - \xi_j$ between the interacting states. To describe the emerging phenomenology, we employ a simplistic model of the spatial structure of matrix elements that assumes each single-particle state i to be effectively connected to a *constant* number Z of states chosen at random from within the localization volume of i. The value of Z can be estimated as a small fraction of the total number of states within the localization volume that has significant spatial overlap with a given state i, so $Z \sim nV_{\rm loc} \times \eta$, where n is the electron concentration and η is a small numerical factor. Due to the proximity to the Anderson transition, the localization volume $V_{\rm loc}$ is large [27, Sec. 2], thus also rendering $Z \gg 1$, even despite the smallness provided by η. We note, however, that for the analysis presented below it is only important that Z itself is a large quantity. In particular, the analysis of a model where each site has the value of Z distributed according to Poisson distribution suggest that the fluctuations of Z do not play a significant role in the observed behavior.

In what follows, we will also retain the information about the energy dependence $D(\xi_i - \xi_j)$ of the matrix elements of the interaction. This energy dependence is primarily characterized by the large energy cutoff ε_D that is typically of the order of the Debye energy of phonons. Due to this energy scale, the interaction between the states with energy difference $|\xi_i - \xi_j|$ larger than ε_D is essentially absent. On the other hand, we assume that the localization volume of single-particle electron states is large enough to secure the continuity of phonon spectrum, i.e., $\delta_{\rm loc} \ll \varepsilon_D$, with $\delta_{\rm loc}$ being the characteristic phonon level spacing in the localization volume. It is worth mentioning that the actual profile of D for dirty superconductors with pseudogap is known to exhibit substantial dependence at small energies due to the underlying phenomenology of Anderson insulator [27, Sec. 4]. This feature presents an additional complication which does not seem to be universally relevant. We will thus simplify the model below by assuming that D is smooth in the vicinity of the zero energy difference and arranges a small static coupling constant $D(0)$. The latter is then conventionally parametrized by small dimensionless Cooper constant $\lambda \ll 1$ as $D(0) = \lambda/(2\nu_0 Z)$, where the multiplier Z in the denominator ensures proper normalization of the matrix element.

An important issue is related to the spatial geometry of the manifold spanned by the indices of eigenstates $i, j, \ldots$, etc. On the one hand, the eigenstates $\psi_i(\boldsymbol{r})$ are supposed to be localized in the physical 3D space (or in the effectively 2D space in case of very thin films), and the locations R_i of the maxima in the absolute values $|\psi_i(\boldsymbol{r})|$ constitute a set of points in real 3D (or 2D) space. On the other hand, the major role in the formation of the superconducting state is played specifically by the eigenstates close to the Fermi level and *in addition* also sufficiently strongly coupled to each other. Since coupling amplitudes between eigenstates near the mobility edge strongly vary in magnitude, only a small fraction of all eigenstates $\psi_j(\boldsymbol{r})$ that can be found around the selected one—$\psi_i(\boldsymbol{r})$—is coupled to $\psi_i(\boldsymbol{r})$ considerably. The resulting spatial structure of *interacting* eigenstates can be considered, in some approximation, as a strongly diluted random graph with some large but finite number of neighbors Z per each participating site. The crucial feature of this graph—as opposed to the usual Euclidean lattice—is its loopless structure. More exactly, a random graph with coordination number Z that is much smaller than the total number of sites N, does contain loops, but their typical size grows with system size as $\sim \ln N/\ln(Z-1)$, while small loops are nearly absent [30]. This, in turn, suppresses infrared fluctuations of the order parameter, which are known to be crucial for the adequate description of thermal phase transitions in low-dimensional systems. On the other hand, in the present problem we are interested in statistical properties of the order parameter at lowest temperatures, where thermal fluctuations are absent anyway. The most important effects to be studied here are due to strong statistical fluctuations (of quenched disorder), which can be considered within the loopless approximation.

B. The model Hamiltonian

The presented phenomenological picture allows us to adopt the following model Hamiltonian of a strongly disordered superconductor on the verge of a localization transition and with a well-developed pseudogap:

$$H = \sum_i \xi_i (a^\dagger_{i\downarrow} a_{i\downarrow} + a^\dagger_{i\uparrow} a_{i\uparrow} + a^+_{j\downarrow} a^+_{j\uparrow} a_{i\uparrow} a_{i\downarrow}) - \sum_{\langle ij \rangle} D_{ij} (a^\dagger_{i\downarrow} a^\dagger_{i\uparrow} a_{j\uparrow} a_{j\downarrow} + \text{Herm. conj.}), \quad (1)$$

and Herm. conj. stands for hermitian conjugate on the first part in the last term. Here, $a^\dagger_{i\sigma}, a_{i\sigma}$ are fermionic creation and annihilation operators of single-particles states $\psi_{i\sigma}$ obeying standard commutation relations, with $\sigma \in \{\uparrow, \downarrow\}$ denoting the spin of the electron. The discussed preformation of Cooper pairs reduces the Hilbert space to eigenstates of Cooper pair occupation number

$$n_i = \tfrac{1}{2}(a^\dagger_{i\downarrow} a_{i\downarrow} + a^\dagger_{i\uparrow} a_{i\uparrow}) = \{0, 1\}, \quad (2)$$

which is obviously conserved by the Hamiltonian. The first term in Eq. (1) then reproduces the randomly distributed independent single-particle energies ξ_i. The corresponding distribution $\nu(\xi)$ has a typical width of order of the Fermi

energy E_F. The particular profile of $\nu(\xi)$ is of little importance for the low-energy physics as long as the single-particle DoS $\nu_0 = \nu(\xi = 0)$ is finite, i.e., $\nu_0 \sim 1/E_F$. The second term in Eq. (1) represents local Cooper-like interaction, with the summation going over all pairs $\langle ij \rangle$ of effectively interacting single-particle states. We assume that each state i is effectively coupled to a large number $Z \gg 1$ of other localized states. Importantly, the pairs of coupled states are chosen completely at random, so the resulting structure bears no information about the original 3D nature of the system (as opposed to similar models that are formulated on a lattice, see, e.g., the 2D-CMF model of Ref. [25]), while also preserving some notion of the translation symmetry (in contrast to the models on a portion of the Bethe lattice, as, e.g., the one of Ref. [23]). The matrix element D_{ij} of the interaction is determined by the energy dependence of the interaction and is modeled by a smooth function with the following asymptotic properties:

$$D_{ij} = D(\xi_i - \xi_j) \approx \begin{cases} \frac{\lambda}{2\nu_0 Z}, & |\xi_i - \xi_j| \lesssim \varepsilon_D \\ 0, & |\xi_i - \xi_j| \gtrsim \varepsilon_D, \end{cases} \tag{3}$$

where $\lambda \ll 1$ is the dimensionless Cooper constant and $\varepsilon_D \ll W$ is the characteristic scale of energy dependence of the Cooper interaction.

C. The self-consistency equation

The superconducting transition for the Hamiltonian Eq. (1) is captured by the saddle-point (Bogolyubov) approach. According to it, one approximates the Cooper interaction with coupling to the field of the complex order parameter Δ. The latter is then found as a minimum of the self-consistent free energy. In the absence of time-reversal symmetry-breaking factors, such as magnetic field or external current, the field of the order parameter Δ_i can be chosen to be real and positive. One then determines the zero-temperature configuration of the order parameter as a positive solution to the following self-consistency equation [27, Secs. 4.3 and 6.1]:

$$\Delta_i = \sum_{j \in \partial i} D(\xi_i - \xi_j) \frac{\Delta_j}{\sqrt{\Delta_j^2 + \xi_j^2}}, \tag{4}$$

where the summation in the right-hand side goes over Z states labeled with index j that interact with a given state i. The reader can find the derivation of this equation for the original Hamiltonian Eq. (1) in Sec. A of the SM [26]. One then has to solve Eq. (4) for a given realization of random energies ξ_i and subsequently analyze the statistical properties of the resulting ensemble of Δ_i, such as the local probability distribution and the structure of spatial correlations.

However, the conventional self-consistent approach fails to describe the SIT itself, namely, Eq. (4) posses nontrivial solutions for arbitrary weak Cooper coupling strength, while in reality one observes destruction of the global superconducting order at a certain value of the coupling constant [23]. The correct description of the SIT requires careful treatment of the self-action of the order parameter in a form of the so-called Onsager reaction term. References [22,23] provide a consistent account for this effect by means of the cavity method [31,32] and demonstrate the emergence of broad probability distributions of the order parameter with slow power-law decay at large values, thus revealing the defining role of extreme values in the corresponding quantum phase transition. However, Ref. [23] also demonstrates that the effects of self-action are only relevant for $Z \lesssim Z_1$, where

$$Z_1 = \lambda \exp\left\{\frac{1}{2\lambda}\right\}, \tag{5}$$

with $\lambda \ll 1$ being the dimensionless Cooper coupling constant. Away from this region, the reaction term constitutes only a small correction, rendering the self-consistency Eq. (4) applicable. We will thus limit our analysis to the case $Z \gtrsim Z_1$, although our technique could be extended to include the Onsager reaction term. Despite the introduced limitation, we report a broad region of Z values for which the distribution of the order parameter still assumes a substantially non-Gaussian profile indicative of the competition between strong fluctuations and global superconducting order.

D. Mean-field solution

The typical scale of the order parameter in Eq. (4) can be established by a simple mean-field approach, namely, one seeks a spatially uniform solution $\Delta_i = \Delta_0 = \text{const}$, approximating the right-hand side of the self-consistency Eq. (4) by its statistical average. This substitution is justified *a priori* for sufficiently large values of Z by virtue of the central limit theorem. As suggested by a seminal paper [28], a physical estimate for the relevant range of Z could be obtained by demanding that each single-particle state has at least one other resonant state within the energy interval of size Δ_0. This results in the following criteria:

$$Z \gtrsim Z_2 = \frac{1}{2\nu_0 \Delta_0} \sim 2\nu_0 \varepsilon_D e^{1/\lambda}. \tag{6}$$

In this case, one can neglect the fluctuations of the right-hand side of Eq. (4) around its mean value and obtain

$$\Delta_0(\xi_0) = Z \left\langle \frac{\Delta_0(\xi)}{\sqrt{\Delta_0^2(\xi) + \xi^2}} D(\xi - \xi_0) \right\rangle_\xi, \tag{7}$$

where $\langle \bullet \rangle_\xi$ denotes the statistical distribution with respect to the distribution of ξ. The equation still contains the value ξ_0 of the disorder field at a given site, reflecting the fact that the order parameter is itself a function of on-site energy ξ_0.

The value of Δ_0 is found self-consistently by solving the resulting integral equation. The smallness of the coupling $D(\xi) \sim \lambda/(2\nu_0 Z)$ at small energies $|\xi| \ll \varepsilon_D$ enables one to provide an analytical solution for the order parameter close to the Fermi surface in a form of the celebrated BCS expression,

$$\Delta_0(\xi_0 = 0) = 2E_0 \exp\left\{-\frac{1}{\lambda}\right\}, \tag{8}$$

where the value of $E_0 \sim \varepsilon_D$ is expressed via the single-particle DoS $\nu(\xi)$ and the exact profile of the D function. The explicit form for E_0 is presented in Sec. A of the SM [26].

As this point, it is worth introducing one more microscopic parameter that turns out to play the defining role for the

distribution of the order parameter:

$$\kappa = \frac{\lambda}{Z/Z_2} \equiv \frac{D(0)}{\Delta_0}. \tag{9}$$

Qualitatively, this parameter combines the information about the criteria Eq. (6) and the strength of the attractive interaction in the form of the dimensionless coupling constant λ. Otherwise, the value of κ bears the meaning of a properly rescaled matrix element of bare attractive interaction. A particularly important aspect of this parameter is that it quantifies the competition between the superconducting pairing and the disorder. The former enters the expression via the value of the bare matrix element of the attraction and the latter is represented by the mean field of the order parameter which is defined by the distribution of the on-site disorder according to Eq. (7).

While our analysis shows that the mean-field result Eq. (8) is only justified for $Z \gtrsim Z_2$, the exponential smallness of the actual order parameter rests solely on the smallness of the coupling constant λ. This makes Δ_0 a valid scale to describe the typical magnitude of the true solution to the self-consistency Eq. (4) in the whole range $Z \gtrsim Z_1$ we are interested in. Below we find distribution function $P(\Delta)$ and show that it can be strongly non-Gaussian in general, while narrow Gaussian shape is realized if the inequality Eq. (6) is satisfied.

E. Relation to previous studies

Our analytical approach presented below in Sec. III borrows certain features from the methods that are widely used to analyze statistical physics of disordered systems on the Bethe lattice. The latter is defined as an infinite tree with all but one vertice having $Z-1$ descendants and one ancestor, while the root site has Z descendants and no ancestor, so each vertex has exactly Z neighbors in total. One of the key properties of the Bethe lattice is the absence of loops, which enables one to derive recursive relations for both a given local quantity itself and distribution function of this quantity across various disorder realizations. Qualitatively, such a possibility can be perceived as a consequence of the fact that in a system with no loops, any two nonoverlapping subsystems are connected by a single chain of sites that arranges the exchange of statistical information and thus induces statistical correlations. This allows one to analyze the statistical properties of the system by considering the state of just a single site. A prominent exploitation of this feature was provided by Mézard and Parisi within their analysis of spin-glass problems on the Bethe lattice [31,32] by means of the cavity method. A similar approach was used in Ref. [23] for a model of a strongly disordered superconductor that is structurally similar to the one used in the present paper.

However, one should be careful when using a finite portion of the Bethe lattice as a model for any physical system. The issue is that truncating the Bethe lattice explicitly breaks the equivalence between different vertices in the system and thus induces a certain preferred direction in the system. Precisely for this reason, we use the ensemble of random regular graphs (RRGs) and its generalizations as a finite size approximation to the Bethe lattice. The important difference between the two structures is that a typical RRG inevitably contains large loops with lengths of the order of the graph's diameter $D \sim \ln N/\ln(Z-1)$ that serve to restore the translation symmetry in the system [30]. Remarkably, our theoretical and numerical analysis shows that as long as the number of neighbors Z of each site is large enough and the disorder is not critically strong (in the sense of the vicinity of the SIT), neither the presence of even short loops nor even the irregularity of the base graph (in the sense that each site might have different number of neighbors) have any noticeable influence on the distribution of the order parameter.

It is worth discussing two more subtle differences between our present approach and the one used previously in Ref. [23]. The cavity method [31,32] was developed originally for Ising-type problems. Relying on the exact recursive relation for the conditional partition function, it derives its power from the possibility to parametrize the latter in terms a local field h_i defined for each site of the problem. This is possible for the classical Ising problem where only two classical states per site are present. Upon taking into account the normalization condition, we are left with only one real number h_i that parametrizes the conditional partition function. Our superconducting problem is different in two aspects. One of them is due to the quantum nature of local degrees of freedom, as already discussed in Ref. [23], namely, the Hamiltonian Eq. (1) can be exactly mapped on the spin-1/2 XY model in transverse field, with the corresponding spin degrees of freedom termed pseudospins [28]. Reference [23] then uses the static approximation that neglects dynamic correlations between pseudospins. The second feature (left unnoticed in Ref. [23]) is that, even with quantum effects neglected, the conditional partition function for a spin-1/2 degree of freedom with XY symmetry cannot be parametrized, in general, by a single complex field Δ_i.

A generalization of the cavity method is certainly possible for this type of order parameter as well, but it is more involved. The difference between the cavity mapping used in Ref. [23] and the exact one becomes important once the terms nonlinear in the magnitude of the order parameter become essential for physics. We expect that the recursive equations derived and analyzed in Ref. [23] are exact (leaving aside the additional problem with the accuracy of the static approximation) as long as the amplitude of the order parameter is small in some appropriate sense. For example, the linearized form of these equations is perfectly suitable, e.g., for the analysis of the temperature-driven transition. It is also correct to use the recursive equations of Ref. [23] for the analysis of the long tail of the order parameter distribution, as the effects of nonlinearity are also weak in this case. In the present paper, we are interested in the shape of the complete distribution function $P(\Delta)$ at $T=0$, where the effects of nonlinearity are strong. Thus, here we prefer to employ a classical form of the self-consistency Eq. (4); as explained in the previous subsection, the related inaccuracy (as long as we do not include Onsager reaction term) is small as the ratio $Z_1/Z \ll 1$.

III. DISTRIBUTION OF THE ORDER PARAMETER

In this section, we present both analytical and numerical results for the on-site joint probability distribution of fields ξ

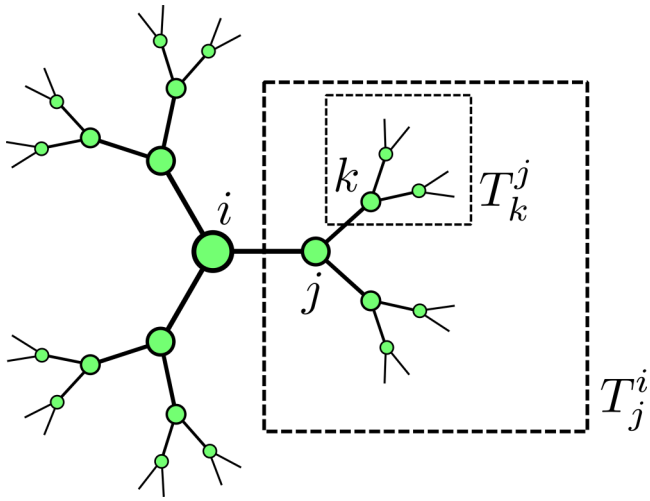

FIG. 1. A schematic illustration of the neighborhood of radius $d = 3$ of a particular vertex i of a random regular graph (RRG) of degree $Z = 3$, i.e., with each vertex having exactly three neighbors. Large RRGs are known to exhibit vanishing concentration of short loops [33], so up to some large distance d the neighborhood of i represents a loop-free structure, i.e., a tree. In particular, each neighboring vertex j is a root of the corresponding branch T_j^i consisting of all vertices that can be reached from i by a path containing at most d edges. Because the whole neighborhood is a tree, such path is unique. Similarly, each nearest neighbor of j except i itself is also a root of a tree T_k^j nested in T_j^i. Such a nested structure is convenient for various recursive considerations.

and Δ on a given site. The latter is defined as

$$P_i(\xi, \Delta) = \langle \delta(\xi - \xi_i)\delta(\Delta - \Delta_i(\{\xi\}))\rangle, \tag{10}$$

where $\delta(x)$ is the Dirac δ function, $\Delta_i(\{\xi\})$ is the exact solution of the self-consistency Eq. (4) for a given realization of the disorder field ξ, and the average $\langle\bullet\rangle$ is performed over all configurations of the ξ field. The distribution is normalized by definition

$$\int_0^\infty d\Delta' P(\xi, \Delta') = \nu(\xi), \tag{11}$$

where $\nu(\xi)$ is the distribution of the original on-site disorder field ξ.

A. Equation on the distribution in a locally treelike system

Within our model, each single-particle state i is effectively interacting with Z other single-particle states selected at random. The corresponding structure of the matrix elements can be represented by an instance of so-called RRGs. The latter are known to exhibit vanishing concentration of finite loops in the thermodynamical limit [33]. In other words, the sites at distances up to some large distance d from any chosen site i form a regular loop-free structure rooted at i with probability approaching unity as the total number of sites N tends to infinity. A fragment of the corresponding structure termed locally treelike is illustrated in Fig. 1.

For the physical system in question, one expects that the spatial distribution of the order parameter exhibits a finite correlation radius, at least away from the SIT. This implies that the value of the order parameter at a given site is only sensitive to the characteristics of neighboring sites up to some finite correlation distance d_0 away from the chosen site. In conjunction with the locally treelike structure, this property suggests that for each site i the neighboring sites $j \in \partial i$ are only correlated via site i itself. Indeed, the underlying graph only contains large loops that are much longer than the correlation length d_0, and thus cannot influence distributions of any local quantities.

To make use of the described properties, we consider the system where the values of both ξ and Δ at a given site i are fixed externally, i.e., $\Delta_{i_0} = \Delta_0$ and $\xi_{i_0} = \xi_0$, as opposed to finding Δ_i from the self-consistency Eq. (4) for site i. Now, consider a nearest neighbor $j \in \partial i$ of the quenched site i. Due to the aforementioned structure of spatial correlations, the exact solution $\Delta_j^i(\{\xi\}|\xi_0, \Delta_0)$ to the modified version of the self-consistency Eq. (4) depends considerably only on the values of the disorder field ξ within some finite region T_j^i rooted at j, see Fig. 1. Crucially, the described locally treelike structure implies that for different j the corresponding essential regions T_j^0 are nonoverlapping. This translates to the fact that the pairs (ξ_j, Δ_j) for various $j \in \partial i$ are rendered uncorrelated in the modified problem, as they are determined by nonoverlapping regions.

Similarly to the initial problem, we are interested in the joint distribution of Δ and ξ for site j in the nearest neighborhood of i for the case when both Δ and ξ at site i itself are fixed externally. The corresponding distribution function is defined as

$$P_j^i(\xi_1, \Delta_1|\xi_0, \Delta_0) = \left\langle \delta(\xi_1 - \xi_j)\delta\left(\Delta_1 - \Delta_j^i(\{\xi\}|\xi_0, \Delta_0)\right)\right\rangle, \tag{12}$$

where $\Delta_j^i(\{\xi\}|\xi_0, \Delta_0)$ is the exact solution of the self-consistency Eq. (4) for a given realization of the disorder field ξ and a fixed value Δ_0 of the order parameter at site i. The average $\langle\bullet\rangle$ is now performed over the values of ξ at all sites except i, where the disorder field assumes the value of ξ_0. The new distribution function is properly normalized, i.e.,

$$\int_0^\infty d\Delta_1' P_j^i(\xi_1, \Delta_1'|\xi_0, \Delta_0) = \nu(\xi_1), \tag{13}$$

valid for any ξ_0, Δ_0, ξ_1. The aforementioned partition of the neighborhood of i into nonoverlapping treelike structures T_i^j then translates to the fact that the averaging in Eq. (12) only reflects the statistical fluctuations of ξ in the corresponding region T_i^j originating from the site j of interest.

The local structure of the problem along with the above outlined statistical independence of different neighbors $j \in \partial i$ in the modified problem allows one to connect the on-site distribution $P_i(\xi_0, \Delta_0)$ at site i with the distributions P_j^i in the modified problem. To this end, one uses the self-consistency Eq. (4) for site i. On the one hand, it is trivially satisfied by the exact solution $\Delta_i(\{\xi\})$ to the *original* problem. On the other hand, the values of Δ_j are given by the solutions $\Delta_j^i(\{\xi\}|\xi_0, \Delta_0)$ to the *modified* problem for a consistent choice of the values ξ_0, Δ_0. In other words, letting $\Delta_j = \Delta_j^i(\{\xi\}|\xi_0, \Delta_0)$ with $\xi_0 = \xi_i$, $\Delta_0 = \Delta_i$ produces an equation on the value of Δ_i itself. These two observations valid for any disorder realization can be translated to the following

relation between the two problems:

$$P_i(\xi,\Delta) = P_i(\xi)\int_{-\infty}^{\infty}\frac{d\tau}{2\pi}\times\frac{\partial}{\partial\Delta}\left\{\left(\int_E^{\Delta} d\Delta' e^{-i\tau\Delta'}\right)\prod_{j\in\partial i}\left(\int d\xi_j d\Delta_j \times P_j^i(\xi_j,\Delta_j|\xi,\Delta)e^{i\tau f(\xi_j,\Delta_j|\xi)}\right)\right\}. \tag{14}$$

Here, $P_i(\xi)$ is the distribution of the on-site disorder; $f(\xi_j,\Delta_j|\xi)$ represents a shorthand for the right-hand side of the self-consistency Eq. (4):

$$f(\xi_j,\Delta_j|\xi) = \frac{\Delta_j}{\sqrt{\Delta_j^2+\xi_j^2}}D(\xi_j-\xi). \tag{15}$$

The lower integration limit E in the integral over Δ' can be set to an arbitrary positive constant. While the value of the whole expression does not depend on E due to normalization of the probability distribution P_j^i, one can use various values of E to simplify the calculations. The specific structure of the equation is due to the fact that computing a distribution of solutions to a given equation with disorder requires taking into account the Jacobian resulting from replacing the δ function of the solution with a δ function of the corresponding equation. The detailed derivation of Eq. (14) is presented in Sec. B of the SM [26].

In a similar fashion, one can formally consider quenching site j as well and determining the resulting on-site distribution $P_k^j(\xi_2,\Delta_2|\xi_1,\Delta_1)$ for some $k\in\partial j\backslash\{i\}$, i.e., next-to-nearest neighbor of the initial site i. It is important that due to the treelike structure, the distribution P_k^j receives no information about the values of field ξ and Δ at the initial site i. The same considerations as the one that lead to Eq. (14) then allow one to connect the on-site distribution P_j^i of site j with those on all nearest neighbors of j except i itself:

$$P_j^i(\xi_1,\Delta_1|\xi_0,\Delta_0) = \nu(\xi_1)\int_{-\infty}^{\infty}\frac{d\tau}{2\pi}\times\frac{\partial}{\partial\Delta_1}\left\{\left(\int_E^{\Delta_1} d\Delta_1' e^{-i\tau\Delta_1'+i\tau f(\xi_0,\Delta_0|\xi_1)}\right)\right.$$
$$\left.\times\prod_{k\in\partial j\backslash\{i\}}\left(\int d\xi_k d\Delta_k \times P_k^j(\xi_k,\Delta_k|\xi_1,\Delta_1)e^{i\tau f(\xi_k,\Delta_k|\xi_j)}\right)\right\}. \tag{16}$$

The final step of the derivation is to exploit translational and rotational symmetries of the underlying graph, as the latter are restored after averaging over disorder. In other words, the choice of i and $j\in\partial i$ is arbitrary, so translational invariance implies independence of both the original P_i and the modified P_j^i distributions on the choice of i, while rotational invariance suggests that P_j^i is the same for all $j\in\partial i$. This allows one to replace all P_j^i with just a single function P_1, arriving at the central results of this section:

$$P(\xi,\Delta) = \nu(\xi)\int_{-\infty}^{\infty}\frac{d\tau}{2\pi}\frac{\partial}{\partial\Delta}\left\{\left(\int_E^{\Delta} d\Delta' e^{-i\tau\Delta'}\right)\left(\int d\xi_1 d\Delta_1 \times P_1(\xi_1,\Delta_1|\xi,\Delta)e^{i\tau f(\xi_1,\Delta_1|\xi)}\right)^Z\right\}, \tag{17}$$

$$P_1(\xi_1,\Delta_1|\xi_0,\Delta_0) = \nu(\xi_0)\int_{-\infty}^{\infty}\frac{d\tau}{2\pi}\frac{\partial}{\partial\Delta_1}\left\{\int_E^{\Delta_1} d\Delta_1' \exp\{-i\tau\Delta_1'+i\tau f(\xi_0,\Delta_0|\xi_1)\}\right.$$
$$\left.\times\left(\int d\xi_2 d\Delta_2 \times P_1(\xi_2,\Delta_2|\xi_1,\Delta_1)e^{i\tau f(\xi_2,\Delta_2|\xi_1)}\right)^{Z-1}\right\}. \tag{18}$$

Both expressions Eqs. (17) and (18) preserve the normalization of the distributions, as can be checked by direct computation.

The accuracy of Eqs. (17) and (18) is governed by the presence of small loops in the system. However, the relative magnitude of the corresponding corrections is estimated as $\sim Z^{-l}$. This estimation originates from the fact that correlations in the distribution of Δ can be shown to decay as Z^{-d}. Because of the aforementioned loopless structure of large regular graphs, Eqs. (17) and (18) become exact in the thermodynamical limit. In reality, however, finite loops are present in the system, but their concentration is typically small [33], rendering their physical effect insignificant. Our additional numerical experiments show that for sufficiently large Z even the shortest loops of length three do not cause any noticeable deformation of the on-site distribution functions, namely, the empirical distribution of the order parameter on those sites that are members of any cycle of length three in the graph is statistically indistinguishable from the probability distribution for the remaining fraction of sites.

We also note that our approach allows a systematic computation of any other joint probability distribution functions for any group of sites of finite spatial size. In particular, a joint probability distribution $P_{ij}(\xi_i,\Delta_i;\xi_j,\Delta_j)$ for any two sites at

some finite distance d is expressible in terms of certain integrodifferential transform of the product of two P_1 functions. It is worth noting at this point that both the direct inspection of our approach and the answer for the joint probability distribution for the two neighboring sites i and $j \in \partial i$ suggest that P_1 *does not* coincide with a conditional distribution function of the form $P_{ij}(\xi_i, \Delta_i; \xi_j, \Delta_j)/P_i(\xi_i, \Delta_i)$. Although the two objects share some qualitative properties, they are in fact quite different quantitatively. The difference can be traced down to the aforementioned Jacobian originating from representing the δ function of the solution in terms of the δ function of the original equations.

We conclude this subsection by noting that the developed formalism allows numerous extensions of the form of the f function. As long as the underlying physical assumptions of conditional statistical decoupling (i.e., the locality of correlations) hold true, the exact form of the right-hand side of the analyzed Eq. (4) is of little importance. Possible generalizations include the effects of finite temperature and other types of uncorrelated disorder. In particular, Sec. G of the SM [26] presents analysis of a more general model that reflects mesoscopic fluctuation in the values of the matrix elements between localized electron states. The key qualitative changes to our results due to such fluctuations are summarized in Sec. III G.

B. The limit of small Δ and large Z

Having Eqs. (17) and (18) at hand, it is now our aim to simplify the equations to reflect the fact that the typical scale of the order parameter is the only relevant energy scale in the problem. In other words, we want to exploit the hierarchy of scales of the form $\Delta \ll \varepsilon_D, E_F$ that is naturally present in the problem. By carefully expanding Eqs. (17) and (18) according to this relation of scales, we will eventually be able to solve Eq. (18) for P_1 and calculate the resulting distribution $P(\xi, \Delta)$ by means of Eq. (17).

We start by introducing the following dimensionless quantities:

$$x_i = \frac{\xi_i}{\Delta_0}, \quad y_i = \frac{\Delta_i}{\Delta_0}, \tag{19}$$

where Δ_0 is the mean field value of the order parameter defined in Sec. II D. Similarly to the conventional theory of superconductivity, we then expect that the high-energy physics playing out at scales ε_D, E_F does not find its way in the low-energy physics, as the sole role of higher energies is to dictate the overall scale of superconducting correlations.

Equation (18) suggests the following quantity as a proper object in the limit of small Δ:

$$m(S|x,y) := \ln\left\{\left[\int d\xi_1 d\Delta_1 \times P_1(\xi_1, \Delta_1|\xi, \Delta) \exp\{iSf(\xi_1, \Delta_1|\xi)/\Delta_0\}\right]^{Z-1}\right\}, \quad \xi = \Delta_0 x, \quad \Delta = \Delta_0 y. \tag{20}$$

It represents a dimensionless form of the cumulant generating function for the right-hand side of the self-consistency Eq. (4) for site j in the modified version of the problem; see the detailed description in the preceding Sec. III A. In particular, the normalization condition Eq. (13) translates to the following trivial identity:

$$m(0|x,y) = 0, \tag{21}$$

valid for any x, y.

The integrodifferential Eq. (18) can be reformulated in terms of m function in a straightforward fashion. The proper low-energy limit of this equation consists of formally retaining only the leading orders in powers of small parameters $\nu_0\Delta_0$, $1/Z \ll 1$ while treating their product as a finite constant $Z_{\text{eff}} = 2\nu_0\Delta_0(Z-1)$ that may attain any numerical value, either large or small. The physical meaning of Z_{eff} is the *effective* number of interacting neighbors, that is, pairs with local energies within the energy stripe of width $\sim\Delta$. Evidently, local fluctuations of the order parameter will be small if $Z_{\text{eff}} \gg 1$. A proper reduction of Eq. (18) to the low-energy sector of the theory should be implemented with care due to logarithmic divergency at high energies, with the latter being typical for any kind of BCS-like theory. Working out a proper cutoff for this divergence requires certain technical effort. The corresponding technical details are described in Sec. C of the SM [26] for a simple case of trivial energy dependence of the matrix element, i.e., $D(\xi) = D(0) = \text{const}$. Although not exactly physical, the latter case showcases all insights necessary to obtain a controlled limit of small Δ_0. Section F of the SM [26] then describes the generalization of the approach to the case of smooth $D(\xi)$ with some finite energy scale of the order of the Debye energy ε_D. Below we formulate the outcome of this procedure.

The $m(S|x,y)$ function possesses the following parametrization that is natural to describe the effects resulting from carefully processing the aforementioned logarithmic behavior in the theory,

$$m(S|x,y) = iSm_1(w) + m_2(S|w), \tag{22}$$

$$w = \omega(z = x/y) = \frac{1}{\sqrt{1+z^2}}, \tag{23}$$

valid for $|x| \leqslant x_{\max}$, where $x_{\max} \sim \varepsilon_D/\Delta_0 \gg 1$ by assumption. The function m_2 is constructed in such a way that its expansion in powers of small S starts from the second order, i.e., $m_2(S|w,x) = O(S^2)$ for $S \ll 1$. For both m_1, m_2, the w arguments assumes values in $[0, 1]$. The functions m_1, m_2 then satisfy the following pair of integrodifferential

equations:

$$m_1(w) = m_1(0) + \kappa w\alpha + \lambda \int_0^1 dw_1 \sqrt{1-w_1^2}\frac{m_1(w_1)-m_1(0)}{w_1} + \lambda \int_0^\infty dy_1 y_1 \ln\frac{1}{y_1}\int_{\mathbb{R}-i0}\frac{ds}{2\pi}\exp\{is\kappa w\}\exp\{m(s|0)-isy_1\}, \tag{24}$$

$$m_2(S|w) = \lambda \int_0^1 dw_1 \frac{\exp\{iS\kappa w_1\}-1-iS\kappa w_1}{w_1^2\sqrt{1-w_1^2}}\left[1-w_1\left(1-w_1^2\right)\frac{\partial}{\partial w_1}\right]\left[\frac{\kappa w + m_1(w_1)}{\kappa}\right]. \tag{25}$$

These equations constitute a proper low-energy limit of Eq. (18). The result contains three controlling parameters λ, κ, α that define the form of the solution and are themselves defined by high-energy physics. By definition, $\lambda = 2\nu_0 ZD(0)$ is the dimensionless Cooper attraction constant, the parameter κ is defined as

$$\kappa = \frac{\lambda}{2\nu_0\Delta_0(Z-1)} = \frac{\lambda}{Z_{\text{eff}}}, \tag{26}$$

and the value of α is given by the following expression:

$$\alpha = 1 + \lambda \int_{\mathbb{R}} \frac{d\xi\,\nu(\xi)}{2\nu_0}\times\frac{D(\xi)}{D(0)}\times\frac{D(\xi)-\mathcal{D}(\xi)}{D(0)|\xi|}, \tag{27}$$

where the $\mathcal{D}$ function is the solution to the following integral equation:

$$\mathcal{D}(\xi_0) = D(\xi_0) + \lambda\int\frac{d\xi\,\nu(\xi)}{2\nu_0}\frac{D(0)D(\xi-\xi_0)-D(\xi_0)D(\xi)}{D^2(0)|\xi|}\mathcal{D}(\xi). \tag{28}$$

The physical sense of $\mathcal{D}$ is to reflect the mean-field energy dependence of the order parameter at scales $\xi \sim \varepsilon_D$, namely, it describes the behavior of the solution $\Delta(\xi) = \Delta_0\mathcal{D}(\xi)$ to the mean-field Eq. (7), see Sec. A of the SM [26] for details. As already mentioned above, the derivation of these results is presented in Sec. C of the SM [26] for the simple case with $D(\xi) = D(0) = \text{const}$ and in Sec. F of the SM [26] for the case of smooth D. The resulting expressions are applicable as long as the actual value of the order parameter $\Delta \sim \Delta_0$ is much smaller than any other typical scale in the problem.

The solution to Eqs. (27) and (28) renders the value of α that is close to unity as long as the coupling constant λ is small enough:

$$\alpha \approx 1 + \lambda^2 c, \quad c \sim 1. \tag{29}$$

Furthermore, the exact values of both α and λ provide only a certain quantitative effect, while the only essential role in the statistics of the order parameter belongs to the parameter κ. In particular, in the following Sec. III D it is shown that large values of κ correspond to heavily non-Gaussian regime of the distribution, while the region $\kappa \ll 1$ reproduces the Gaussian statistics as it corresponds to the region defined by Eq. (6).

Once the solution to Eqs. (24) and (25) is obtained, one uses the expression Eq. (17) to calculate the joint probability distribution $P(x, y)$ of the fields $x = \xi/\Delta_0$ and $y = \Delta/\Delta_0$,

$$P(x,y) = P(x)\int_{\mathbb{R}}\frac{ds}{2\pi}\times\frac{\partial}{\partial y}\left\{\left[\int_0^y dy'\exp\{-isy'\}\right]\times\exp\{m(s|\omega(x/y))\}\right\}, \quad \omega(z=x/y) = \frac{1}{\sqrt{1+z^2}}, \tag{30}$$

where all probability distributions are understood in their dimensionless form, so the probability measure is defined as $P(x)dx$, $P(x, y)dxdy$, etc. In particular, the value of $P(x)$ is given by $P(x) = \Delta_0\nu(\xi = \Delta_0 x)$. The expression is valid for $|x| \ll \varepsilon_D/\Delta_0$, while the remaining region is covered in Sec. F of SM [26]. At this point, a comment is in order regarding the qualitative behavior of $P(x, y)$ with respect to the first argument $x = \xi/\Delta_0$. From general physics reasoning, one expects that there are two important regions: $|x| \sim 1$ and $|x| \gtrsim \varepsilon_D/\Delta_0 \gg 1$. In the former, the joint distribution is expected to exhibit nontrivial behavior that is the central topic of this paper. On the contrary, the region of large $|x|$ describes the situation when the Cooper attraction is not effective anymore because the corresponding single-particle state is two far away from the Fermi surface and thus does not contribute to the global superconducting order. As a result, one expects that for $|x| \gtrsim \varepsilon_D/\Delta_0$ the joint probability distribution is concentrated around $y = 0$ and thus bears no physical meaning whatsoever.

The distribution $P(y)$ of the order parameter is then obtained by integrating the joint distribution $P(x, y)$ over x. According to the discussion above, the upper limit of this integration is $x_{\max} \sim \varepsilon_D/\Delta_0$, which corresponds to local site energies close to Fermi level, i.e., $|\xi| \lesssim \varepsilon_D$. The result has the following simple form

$$P_0(y) = \int_{\mathbb{R}}\frac{ds}{2\pi}\exp\{m(s|0)-isy\}. \tag{31}$$

It is now evident that the quantity $m(s|0)$ represents the cumulant generating function of the order parameter, that is,

$$m(s|0) = \ln\left[\left\langle\exp\left\{is\frac{\Delta}{\Delta_0}\right\}\right\rangle\right], \tag{32}$$

where the average $\langle\bullet\rangle$ is taken over the distribution P_0, i.e., only takes into account physically relevant states close to the Fermi surface.

The theoretical approach developed thus far can be summarized as follows. Given the values of the parameters κ, λ, α

defined by high-energy physics according to Eqs. (26)–(28), one solves the system of Eqs. (24) and (25) for the m function. This function alone contains complete information about the statistical properties of the self-consistency Eq. (4). In particular, the very definition Eqs. (20) of the m function implies that the modified distribution $P_1(x_1, y_1|x, y)$ is directly restored from $m(S|x, y)$ by computing the right-hand side of Eq. (18), with the latter being expressible in terms of m alone. One then uses expression Eq. (31) to calculate the on-site probability distribution of the order parameter close to the Fermi surface or a similar expression for joint probability distributions of interest. The latter can be systematically expressed in terms of the $P_1(x_1, y_1|x, y)$ distribution according to the procedure delineated in Sec. III A.

C. Weak coupling approximation $\lambda \ll 1$

It turns out that Eqs. (24) and (25) admit a complete analytical solution for the case of small coupling λ. While we have already used the smallness of the coupling constant in the form of the corresponding exponential smallness of the order parameter to derive Eqs. (24) and (25) themselves, the value of λ in the resulting low-energy theory is not restricted to small values and can itself assume values of the order of unity. For the case of small values of λ, however, we now present a consistent expansion of the m function in powers of small λ that constitutes a full solution to the system Eqs. (24) and (25). A detailed procedure is presented in Sec. E of the SM [26], while this subsection demonstrates the final results.

The leading term of the m_2 function reads

$$m_2(S|w) = \lambda[(w + w_0)\Phi_0(\kappa S) + \Phi_1(\kappa S)], \tag{33}$$

where Φ_0 and Φ_1 are special functions with the following integral representations:

$$\Phi_0(\sigma) = \int_0^1 \frac{dw_1}{w_1^2\sqrt{1-w_1^2}}\{e^{i\sigma w_1} - 1 - i\sigma w_1\}, \tag{34}$$

$$\Phi_1(\sigma) = \int_0^1 \frac{w_1 dw_1}{\sqrt{1-w_1^2}}\{e^{i\sigma w_1} - 1 - i\sigma w_1\}, \tag{35}$$

and w_0 is a constant that is determined below in a self-consistent fashion. The special functions can be expressed in terms of a generalized hypergeometric series, see Sec. E of the SM [26]. One then substitutes this form of the m_2 function in Eq. (24) for the remaining m_1 term. Restoring the functional form of the w dependence up to the same precision as the expression Eq. (33) for m_2 then renders

$$m_1(w) = \kappa(w + w_0) + \lambda\left[(w_0 + w)\ln\frac{1}{w_0 + w} - w_0 \ln\frac{1}{w_0}\right]. \tag{36}$$

Finally, Eq. (24) also produces a self-consistency equation for $m_1(0)$, which allows one to determine the value of w_0:

$$w_0 = w_0^{(0)} + \lambda w_0^{(1)}, \tag{37}$$

$$w_0^{(0)} = \frac{\pi/4}{W(\pi\kappa/4)}, \quad w_0^{(1)} = \frac{\frac{\pi}{4}\ln\frac{1}{\kappa} + F\left(w_0^{(0)}\right)}{\ln\kappa w_0^{(0)} + 1}. \tag{38}$$

where $W(z)$ is the principal branch of the Lambert's W function, and $F(w)$ is a special function with the following integral representation:

$$F(w) = \int_0^1 dw_1 \frac{w_1^2 + \left(1 - w_1^2\right)\ln\frac{1}{w}}{\sqrt{1-w_1^2}} + \int_0^1 dw_1 \frac{(w + w_1)^2 \ln\frac{w}{w+w_1} + w w_1}{w_1^2\sqrt{1-w_1^2}}. \tag{39}$$

Section E of the SM [26] contains an explicit expression for the F function in terms of polylogarithm function $\mathrm{Li}_2(z)$. Equations (33)–(39) thus constitute a complete solution for the m function that is restored from m_1 and m_2 contributions according to Eq. (22). The obtained expressions are then to be used to compute the value of the distribution function $P_0(y)$ by means of Eq. (31). Figure 2 features the resulting theoretical curves along with the ones obtained with the use the exact solution to Eqs. (24) and (25) and with a histogram of direct numerical solution to the original self-consistency Eq. (4).

The applicability of the presented expansion is limited by the subleading terms in λ. The corresponding control parameter is given by

$$\frac{\lambda}{w_0^{(0)}} = \lambda\frac{4}{\pi}W\left(\frac{\pi\kappa}{4}\right) \ll 1, \tag{40}$$

which, in turn, limits the value of the microscopic parameter Z of our model as

$$Z \gg Z^* = \frac{\pi}{4} \times \frac{\lambda}{2\nu_0 \times 2\varepsilon_D}\exp\left\{\frac{1}{\lambda}\left(1 - \frac{\pi}{4}\right)\right\}. \tag{41}$$

Remarkably, the resulting scale of Z is exponentially smaller than the value of $Z_1 = \lambda\exp\{1/2\lambda\}$, which limits the applicability of the original self-consistency Eq. (4) due to the neglect of the Onsager reaction terms, as explained in the discussion after Eq. (5).

We have thus obtained a set of expressions that fully describe the statistics of the order parameter in the entire region of applicability of the original self-consistency Eq. (4), namely, expressions Eqs. (33)–(39) explicitly describe the m function, which, in turn, contains full information about the joint statistics of the order parameter Δ and the disorder field ξ, as explained in Sec. III A.

D. Extreme value statistics

The exact Eqs. (24) and (25) presented earlier admit asymptotic analysis that allows one to extract the behavior of the probability density function $P_0(y)$ of the dimensionless order parameter y in several important limiting cases. These include the limit of the Gaussian distribution of the order parameter that connects our model to the conventional weak disorder limit as well as the extreme value statistics in the regime of non-Gaussian distribution of the order parameter corresponding to moderate and large values of κ.

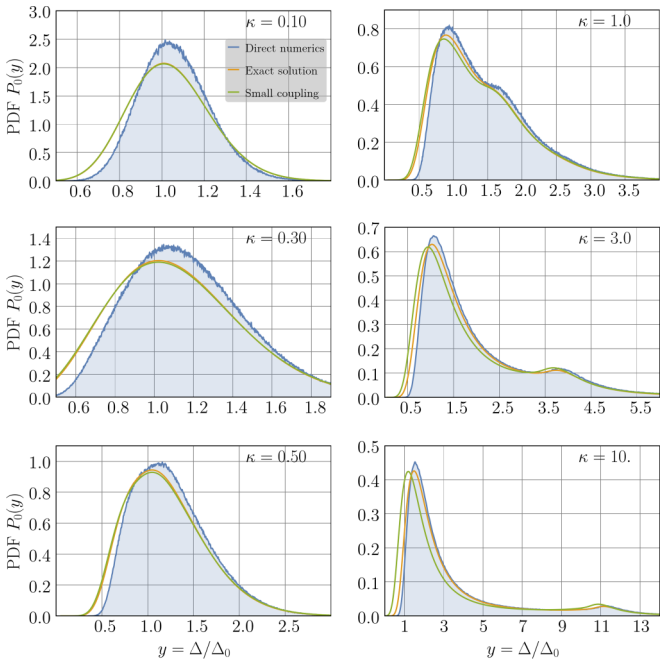

FIG. 2. A series of plots for the probability density function (PDF) of the dimensionless order parameter $P(\Delta/\Delta_0)$ for various values of the parameter κ. The filled blue line is the histogram obtained from direct numerical solution of the self-consistency Eq. (4) on a random regular graph of size $N = 2^{22} \approx 4.2 \times 10^6$. The orange line is obtained by solving Eqs. (24) and (25) for the function $m(S|w)$ and subsequently evaluating the integral Eq. (31) for the distribution function. The green line uses the analytical expressions Eqs. (33)–(39) of Sec. III C to approximate the value of the m function used to compute the integral Eq. (31) for the PDF. For simplicity, the model with $D(\xi) = \text{const}$ is used. Values of $\kappa = \{0.3, 0.5, 1.0, 3.0, 10\}$ are realized in the system with $Z = 51$ and $\lambda \approx \{0.199, 0.177, 0.154, 0.129, 0.110\}$, respectively, and $\kappa = 0.1$ corresponds to $Z = 101$ and $\lambda \approx 0.222$. The last pair of values for Z, λ is motivated by the fact that larger values of λ render large values of Δ, while our theory corresponds to the limit $\nu_0\Delta \ll 1$, with the leading correction being of order $2\nu_0\Delta_0/\lambda \approx (\kappa Z)^{-1}$. That is why to obtain small κ one has to use larger Z so as to keep the value of λ small enough. The aforementioned corrections to small Δ_0 limit are also responsible for the mismatch between the theory and numerical data that is pronounced for $\kappa = 0.1, 0.3$ and is also somewhat observable for larger values of κ with an apparent decreasing trend (the theoretical curves have no fitting parameters). The mismatch between the two instances of the theoretical descriptions originates from corrections of order $\sim\lambda^2$ neglected in the approximate analytical solution (green line), see Sec. III C for details. One can observe the defining role of κ for the profile of he distribution: small κ produce Gaussian regime, while large κ render nontrivial distribution function, whose asymptotic behavior is discussed in Sec. III D.

1. Gaussian regime of weak disorder $\kappa \ll \lambda$

We start by formally considering the limit of large number of neighbors that corresponds to the regime of weak fluctuations. Within our theory, this regime is realized at $\kappa \lesssim \lambda$, in consistence with the physical criteria articulated in Sec. II D. For small values of κ, the integral over s in Eq. (31) for the probability distribution $P_0(y)$ gains its value near the trivial saddle point $s = 0$, as the m function depends on s only via a combination κs. This, in turn, implies that only the two leading terms in the expansion of the m function in powers of small s are important for the value of the integral Eq. (31). As it is shown in Subsec. C4 of the SM [26], these leading terms are straightforwardly extracted from the system Eqs. (24) and (25) and read

$$m(S \ll \kappa^{-1}|w) = \left\{1 + \left(\frac{\pi}{4} + w\right)(1-\lambda)\kappa\right\}(iS), \\ + \frac{1}{2}\lambda\kappa\left\{\frac{\pi}{2} + \left[\frac{\pi^2}{8} + \frac{2}{3}\right](1-\lambda)\kappa + \frac{\pi}{2}\kappa w\right\}(iS)^2. \quad (42)$$

The higher order corrections are negligible for $\kappa S \ll 1$. With this expression at hand, one obtains the following approximate expressions for the probability density function of the order parameter:

$$P_0(y) \approx \frac{1}{\sqrt{2\pi\sigma^2}} \exp\left\{-\frac{(y - \langle y\rangle)^2}{2\sigma^2}\right\}, \quad (43)$$

$$\langle y\rangle = 1 + \frac{\pi}{4}(1-\lambda)\kappa, \quad (44)$$

$$\sigma^2 = \frac{\pi}{2}\lambda\kappa\left\{1 + \left[\frac{\pi}{4} + \frac{4}{3\pi}\right](1-\lambda)\kappa\right\}. \quad (45)$$

As already mentioned, the discussed approximation is valid for $\kappa \lesssim \lambda$, as follows from analysis of higher order corrections to the expansion Eqs. (42), see Subsec. C4 of the SM [26] for details. The presented results Eqs. (43)–(45) are otherwise accessible by a direct averaging of the original self-consistency Eq. (4). Indeed, upon applying the central limit theorem to the right-hand side of Eq. (4), one concludes that the order parameter in the left-hand side obeys a Gaussian distribution Eq. (43) with the parameters given by Eqs. (44) and (45). The region $\kappa \lesssim \lambda$ is thus consistent with the basic expectations in the regime of weak disorder.

2. Strong disorder $\kappa \gtrsim \lambda$, small-y tail

In case $\kappa \gtrsim \lambda$, the full shape of the distribution function $P_0(y)$ cannot be computed analytically in the general case. However, its behavior at both large and small values of y is reproduced by the saddle-point analysis of the corresponding integral Eq. (31). The latter, in turn, requires asymptotic analysis for the m function at large purely imaginary arguments. This asymptotic behavior can be extracted from Eq. (25). A detailed exposition of the procedure is presented in Sec. D of SM [26], while here we only quote the results.

For small values of y, one finds the following asymptotic expression for the probability:

$$P_0(y \lesssim 1) \approx \sqrt{\frac{\zeta(y)}{2\pi[\lambda\langle y\rangle]^2}} \times \exp\{-\zeta(y)\}, \quad (46)$$

with the exponent $\zeta(y)$ given by

$$\zeta(y) = \frac{\lambda\langle y\rangle}{2\kappa} \exp\left\{\frac{1}{\lambda}\left(1 - \frac{y}{\langle y\rangle}\right) - \frac{\langle y \ln y\rangle}{\langle y\rangle} - \gamma\right\}, \quad (47)$$

where $\langle\bullet\rangle$ denotes the mean value with respect to the full distribution $P_0(y)$ itself, and $\gamma = 0.577...$ is the Euler-Mascheroni constant. The expressions Eqs. (46) and (47) are

valid as long as the value of ζ is sufficiently large, viz.

$$\zeta(y) \gg \max\left\{\frac{\lambda\langle y\rangle}{\kappa}, 1\right\}. \tag{48}$$

For the case $\kappa \lesssim \lambda \ll 1$ considered, the condition above reduces to $\zeta \gg 1$. We choose to retain the more general form for the discussion relevant to the case $\kappa \lesssim \lambda$ below.

3. *Strong disorder $\kappa \gtrsim 1$, large-y tail*

In the limit of large values of y, the following asymptotic expression takes place:

$$\ln P_0^{\text{lead}}(y) \sim -\frac{y-\langle y\rangle}{\kappa}\left[\ln\psi + \frac{1}{2}\ln\ln\psi - 1\right] + \ln\left[\frac{1}{\sqrt{2\pi\kappa(y-\langle y\rangle)}}\right], \tag{49}$$

where ψ is a rescaled distance to the mean value,

$$\psi = \frac{y-\langle y\rangle}{\lambda m_1(1)\sqrt{\frac{\pi}{2}}}, \tag{50}$$

with $m_1(1)$ being the exact value of the m_1 function at $w = 1$ given by

$$m_1(1) = \langle y\rangle + \kappa + \lambda\left\langle (y+\kappa)\ln\frac{1}{y+\kappa} - y\ln\frac{1}{y}\right\rangle. \tag{51}$$

The similarity sign $\sim$ in Eq. (49) expresses the fact that the logarithm of the distribution function $\ln P_0(y)$ can be evaluated explicitly only up to subleading corrections of the order $(y - \langle y\rangle)/\ln(y - \langle y\rangle)$. The latter are themselves growing functions of y, which prevents us from evaluating a proper asymptotic form of the P_0 function. A correct expression can only be formulated in terms of the saddle-point approximation that uses the exact form of the m function to estimate the value of the integral Eq. (31). The applicability of the asymptotic form Eq. (49) is controlled by the following condition:

$$y - \langle y\rangle \gg \kappa. \tag{52}$$

We note that while the asymptotic expressions Eqs. (46) and (49) can be used for any value of κ, the corresponding behavior is essentially unobservable for $\kappa \ll 1$. Indeed, in the latter case, the criteria of applicability for the limiting expressions presented above correspond to Eq. (52) for large y and to

$$1 - \frac{y}{\langle y\rangle} \gtrsim \lambda \times \left[\ln 2 + \gamma - \frac{\left\langle y\ln\frac{1}{y}\right\rangle}{\langle y\rangle}\right] \sim \lambda \tag{53}$$

for small y. On the other hand, the Gaussian probability distribution Eq. (43) assumes exponentially small values for

$$|y - \langle y\rangle| \gg \sigma \sim \lambda\kappa. \tag{54}$$

This implies that for the Gaussian regime $\kappa \lesssim \lambda$ the asymptotic expressions Eqs. (46) and (49) only become applicable in the region where the absolute value of the probability is already exponentially small.

4. *Strong disorder $\kappa \gtrsim \lambda$, oscillatory behavior at large y*

The asymptotic expression Eq. (49) does not account for the subleading saddle points in the integral Eq. (31) over s that are present for the case $y > \langle y\rangle$**a**(as discussed in detail in Subsec. D2 of the SM [26]). The total probability is given by a sum over contributions from all saddle points:

$$P_0(y) = P_0^{\text{lead}}(y) + \sum_{n=-\infty}^{\infty} P_0^{(n)}(y), \tag{55}$$

where $P_0^{\text{lead}}(y)$ is the leading contribution described by Eq. (49), and $P_0^{(n)}(y)$ is the subleading term produced by a pair of complex secondary saddle points $z_{-n} = \overline{z_n}$ enumerated by $n \in \mathbb{Z}$. Similarly to the quality of estimation Eq. (49), a proper asymptotic expression for each subleading contribution requires the exact form of the m function. One can provide only the leading log-accurate expression for each of the subleading contributions,

$$\ln\frac{P_0^{(n)}(y)}{P_0^{\text{lead}}(y)} \sim -\frac{y-\langle y\rangle}{\kappa} \times 2\pi i n\left(1 + \frac{1}{2\ln\psi}\right), \tag{56}$$

with ψ defined in Eq. (50). While we are not able to provide an asymptotic expression for the result of the summation due to the poor accuracy of the estimation of the summation terms, even at the level of Eq. (56) one can observe that the resulting probability distribution exhibits oscillations. Indeed, the estimation Eq. (56) indicates that each secondary contribution is close to a periodic function with period $\Delta y = \kappa$. The sum Eq. (55) thus features constructive interference from all contributions at values of y described by

$$y^{(n+1)} - y^{(n)} \approx \kappa, \quad y^{(0)} = \langle y\rangle, \tag{57}$$

where $n \in \mathbb{N}$ enumerates the secondary peak that emerges from the such an interference.

E. Numerical analysis of the problem

In this section, we briefly describe the numerical routines used to analyze both the original self-consistency Eq. (4) and the integral Eqs. (24) and (25) that constitute the core outcome of the theoretical analysis.

One immediate way to gather the statistics of the solution of the self-consistency Eq. (4) is to solve it directly for the values of Δ_i in a number of sufficiently large realizations of the system. To this end, we generate an instance of RRG along with a random set of values ξ_i for each site and then solve the system Eq. (4) by a suitable iterative procedure. The size of the base graph reaches $N = 2^{23} \approx 8.4 \times 10^6$, which allowed us to ensure that the thermodynamic limit in all quantities of interest was achieved. The distribution of on-site disorder field $\nu(\xi)$ only determines the overall superconducting scale and otherwise has little to no effect on any of properly rescaled distributions of the order parameter, in full agreement with the general physics as well as our theory. For this reason, all numerical data quoted below uses the box distribution of the form $\nu(\xi) = \theta(|\xi| - 1)/2$ with $\nu_0 = 1/2$, although other distributions have also been considered and observed to produce identical results in accord with our theoretical expectations. The Fermi energy E_F, being the characteristic scale of the distribution, is always used as the energy unit, so all dimensionfull quantities such as $D(\xi)$ are measured in units of E_F. The numerical routine uses the version of

the model with a trivial energy dependence of the interaction matrix element $D(\xi) = D(0) = \text{const}$, and other models are immediately available. However, both the general physics reasoning and our theoretical analysis (see Sec. F of the SM [26] for details) indicate that there is no practical difference between various profiles of $D(\xi)$ as long as they are smooth on superconducting energy scales, i.e., $D(\xi \sim \Delta) \approx D(0)$.

The key focus of this paper, however, is to use the derived equations to describe the statistics of the order parameter analytically. The remaining technical challenge at this point is to solve the pair of integrodifferential Eqs. (24) and (25) for the m function. While Sec. III C provides an approximate analytical solution in terms of special functions, it is still important to verify the numerical accuracy of this approximation. We designed a certain numerical procedure that iteratively constructs the solution to the integrodifferential Eqs. (24) and (25). The implementation can be found in Ref. [34]; it allows one to obtain the solution in several minutes on a usual laptop. Once the solution is determined either numerically or analytically by means of Eqs. (33) and (39), our routine then provides an efficient way to perform the numerical integration of Eq. (31) to calculate the probability distribution $P(y)$ and other objects of interest, such as the joint probability distribution $P(x, y)$ given by Eq. (30). Various averages over the resulting distribution are then available via either yet another numerical integration or by exploiting the fact that the function $m(S|0)$ represents the cumulant generating function of the $P(y)$ distribution, with both methods being optimized within the routine.

We emphasize that the primary outcomes of our analysis are analytical, while the developed numerical routines are mainly used to confirm the analytical results.

F. Overview of the main results

1. The shape of the distribution at various values of disorder

Figure 2 showcases the results of both procedures for various values of microscopic parameters of the model corresponding to qualitatively different profiles of the distribution function $P_0(y)$. As is evident from both the numerical studies and the analytical solution presented below, the parameter κ plays the defining role in the qualitative form of the solution. Indeed, small values of $\kappa \ll 1$ correspond to the regime of small disorder with a Gaussian distribution of the order parameter, while the opposite case of $\kappa \gtrsim 1$ implies a rather involved non-Gaussian profile of the distribution. The exact form and asymptotic behavior of this strong-disorder profile is described in Sec. III D. In particular, a proper discussion of the apparent secondary maximum in the distribution $P_0(y)$ observed for $\kappa \gtrsim 1$ is provided.

The physical reason behind the existence of diverse profiles of the distribution function $P_0(y)$ is related to the smallness of the Cooper coupling constant λ. As was explained in Sec. II C, the bare number of neighbors Z in our model must be above $Z_1 = \lambda e^{1/2\lambda}$ to substantiate our disregard for the Onsager reaction terms in the original self-consistency Eq. (4). On the other hand, it is only at $Z \gtrsim Z_2 \sim e^{1/\lambda}$ when one observes suppression of local fluctuations of the order parameter due to statistical self-averaging, see Eq. (6) and the associated discussion. The smallness of λ then renders an exponentially large region $Z_1 \ll Z \ll Z_2$ where the distribution of the order parameter assumes a complicated profile presented. Taking for the sake of example $\lambda = 0.2$, we find that $Z_1 \approx 2.5$ and $Z_2 \approx 30$; in terms of the κ parameter defined in Eq. (9), the accessible values range from arbitrarily small κ up to $\kappa \lesssim 10$.

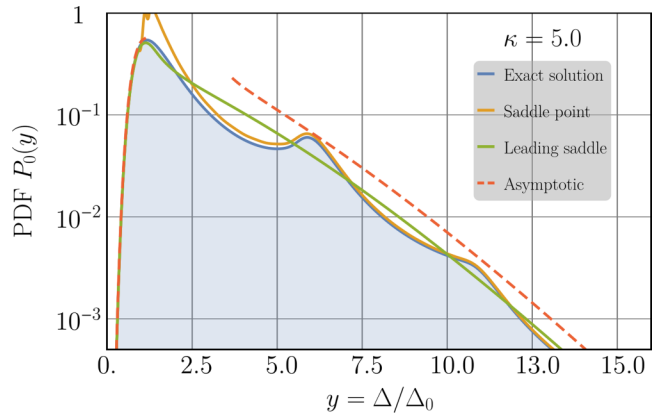

FIG. 3. A log-scale plot reflecting the asymptotic behavior of the probability density function (PDF) of the dimensionless order parameter $y = \Delta/\Delta_0$. The filled blue curve represents the value of the integral Eq. (31) obtained by direct numerical integration. The orange line corresponds to saddle-point approximation of the integral Eq. (31) with all saddle points taken into account for $y > \langle y \rangle$. The green line reflects contribution of the leading purely imaginary saddle point only. When required, the m function is determined from the numerical solution of Eqs. (24) and (25), see Sec. III E for details on the numerical routine. Finally, the dashed red line corresponds to approximate analytic expressions presented in the main Ttext: Eq. (49) for large values of $y > \langle y \rangle$ and Eqs. (46) and (47) for $y < \langle y \rangle$. The microscopic parameters of the model are $D(\xi) = \text{const}$, $\lambda \approx 0.120$, $Z = 51$ and $\kappa = 5.0$. All saddle-point-type approximations naturally fail in the region $y \sim \langle y \rangle$ due to vanishing second derivative at the saddle point. On the other hand, all of them show reasonable agreement with the exact value for both large and small values of y. The discussion of the secondary peaks at large values of y in given in the main text.

2. Asymptotic behavior of the distribution

Figure 3 provides a demonstration of the approximate behavior described by the asymptotic Eqs. (46) and (49) superimposed on the distribution obtained by exact numerical solution of Eqs. (24) and (25) with respect to $m_1(w)$, $m_1(S|w)$ functions (the numerical procedure is explained in Sec. III E). In addition to that, this figure also features the estimations obtained from using the *exact* form of the m function to determine the position of the saddle points and evaluate the resulting approximation of the integral Eq. (31) for the probability density.

We note that the asymptotic form given by Eqs. (46) and (47) for $y < 1$ demonstrates excellent agreement with the exact result. However, the situation is more involved in the opposite limit of large y. The provided approximation Eq. (49) for $y \gtrsim 1$ does describe the asymptotic behavior of the distribution function $P_0(y)$ up to a constant of order unity, in accordance with the quoted accuracy of the corresponding calculation, see the discussion under Eq. (49). On top of that,

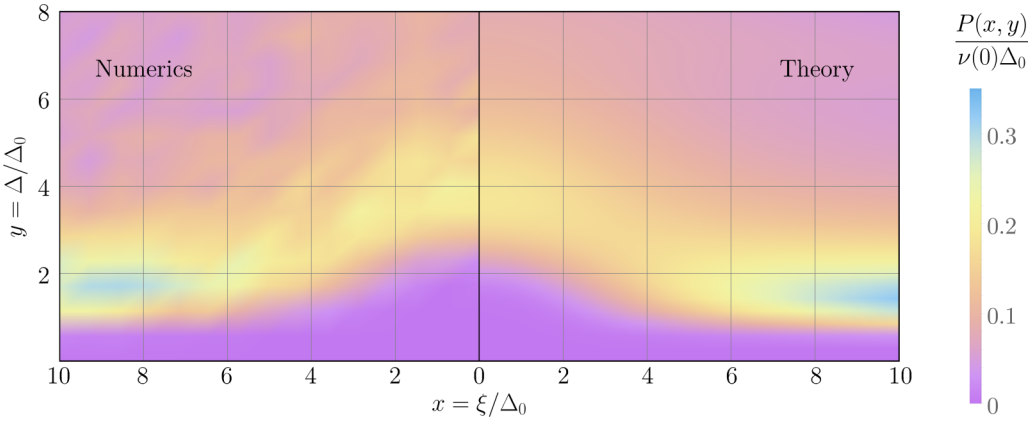

FIG. 4. A color map of the joint probability density function $P(x, y)$ of the on-site values of dimensionless disorder field $x = \xi/\Delta_0$ and dimensionless order parameter $y = \Delta/\Delta_0$ in the vicinity of the Fermi surface corresponding to $\xi = 0$. The color encodes the value of the probability density according to the legend to the right. The left color map corresponds to (smoothened) histogram obtained from direct numerical solution of the original self-consistency Eq. (4), and the right color map reflects the result of the theoretical calculation performed according to expression Eq. (30) with the m function determined from the numerical solution of Eqs. (24) and (25). For simplicity, the model with $D(\xi) = \text{const}$ is used. The parameters of the model in both cases are $\lambda \approx 0.120$ and $Z = 51$, which corresponds to $\kappa = 5.0$. The observed jitter in the results of the direct numerical solution (left plot) is due to the finite size of the corresponding sample: even despite the fact that a system with $N = 2^{22} \approx 4.2 \times 10^6$ sites is used, only $\sim N \times (2\nu_0\Delta_0) \sim 6 \times 10^4$ of them contribute to the presented histogram, resulting in an average of just $\sim$250 points contributing to each bin of the histogram for the chosen bin size $\Delta x = \Delta y \approx 0.71$. The two color maps demonstrate reasonable agreement, simultaneously reproducing several important qualitative features of the joint PDF. In particular, one observes a considerable deformation of the conditional distribution $P_c(\Delta) := P(\xi, \Delta)/P(\xi)$ as $|\xi|$ decreases. See the main text for a detailed discussion.

the oscillations with period $\Delta y = \kappa$ proposed by estimations Eqs. (55) and (56) are also observed.

The observed double-exponential behavior of the probability at $y \leqslant \langle y \rangle$ is secured by a certain type of local disorder configurations. Indeed, one can observe directly from the self-consistency Eq. (4) that the only feasible way to produce an anomalously low value of the order parameter on a given site is to have the values of the disorder fields ξ_j *on all nearest neighbors* larger (in absolute value) than a certain threshold $\xi_{\min} \gg \Delta$. The value of the threshold can be estimated from the mean-field-like treatment of the self-consistency equation and renders $\xi_{\min} \sim \frac{\langle\Delta\rangle}{2} \exp\{\frac{1}{\lambda}(1 - \frac{\Delta}{\langle\Delta\rangle})\}$, and the probability of the such an event to occur in the statistics of ξ is estimated as $P(\min|\xi| > \xi_{\min}) \approx \exp\{-2\nu_0 Z \xi_{\min}\}$ for $Z \gg 1$ and $\xi_{\min} \ll E_F$. Combining these two estimations correctly reproduces the exponential part of Eqs. (46) and (47). A more detailed version of this reasoning is given in Subsec. D1 of the SM [26].

The secondary maxima in the probability distribution $P_0(y)$ also admit a decent physical interpretation in each particular realization of the disorder fields ξ, namely, the nth secondary maximum of the distribution corresponds to the sites with exactly n neighbors with small value of on-site disorder $|\xi_i| \sim \Delta_0$. The apparent sharpness of the peaks can be perceived as a consequence of Van Hove-type singularity in the probability distribution of the terms on the right-hand side of the self-consistency Eq. (4). The latter exhibit a quadratic maximum at $\xi = 0$, and thus possess the probability density that features a square-root singularity as $\xi \to 0$, viz.

$$P\left(\epsilon = \frac{\Delta_0}{\sqrt{\Delta_0^2 + \xi^2}}\right) \approx \frac{\Delta_0}{\sqrt{2(1-\epsilon)}}, \quad \epsilon \to 1. \tag{58}$$

Subsection D3 of the SM [26] describes several quantitative tests to verify this hypothesis at the level of an individual disorder realization. The results are of unequivocal support to the proposed interpretation.

This explanation also suggests that the observed features of the distribution originate from an unphysical assumption that the matrix element of interaction is constant, so the described singularity of Van Hove type is well pronounced. On the other hand, in the real system one naturally expects fluctuations in the coupling matrix element. In the following Sec. III G, we analyze an extension of our model that includes these fluctuations. Our conclusions clearly reflect that the described secondary maxima in the distribution of the order parameter are smeared by fluctuations of the coupling constant.

3. Joint probability distribution

We also present the results for the joint probability distribution $P(x, y)$ of the dimensionless order parameter $y = \Delta/\Delta_0$ and the corresponding on-site local field $x = \xi/\Delta_0$. Figure 4 shows the color maps of the distribution as found from the theoretical approach presented above along with the data obtained from the exact numerical solution of the original self-consistency Eq. (4), as explained earlier. The two pictures indicate a clear agreement up to statistical noise present in the numerical data due to finite sample size.

While the distribution quickly approaches the profile corresponding to the factorized distribution of the form $P_0(y)P(x)$ at sufficiently large values of ξ, there is a noticeable deformation in the region $\xi/\Delta_0 \lesssim 5$ indicative of the strong correlation between the on-site values of ξ and Δ. As can be seen from the original self-consistency Eq. (4), such behavior is a secondary consequence of the fact that a low

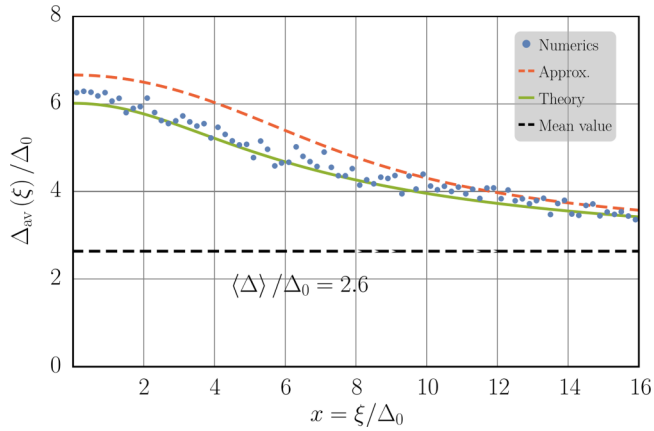

FIG. 5. The plot of the conditional average of the dimensionless order parameter $\Delta_{av}(\xi)/\Delta_0 = \int d\Delta \times \Delta/\Delta_0 P(\Delta,\xi)/P(\xi)$ as a function of on-site value of the dimensionless disorder field $x = \xi/\Delta_0$. The blue points correspond to the result calculated from the direct numerical solution of the self-consistency Eq. (4). The solid green line corresponds to the conditional average computed by direct integration from the theoretical joint probability distribution given by Eq. (30), with the m function determined from the numerical solution of Eqs. (24) and (25). The red dashed line corresponds to physically relevant solution of the approximate Eqs. (59) and (60). Finally, the black dashed line denotes the value of the total average $\langle\Delta\rangle/\Delta_0$ of the dimensionless order parameter as found from both the numerical data and analytic theory. The microscopic parameters of the model are $D(\xi) = \text{const}$, $\lambda \approx 0.120$, $Z = 51$, and $\kappa = 5.0$, so a direct comparison with Fig. 4 is appropriate.

value of ξ at a given site i results in an increase of the order parameter *at all neighboring sites* $j \in \partial i$ by a contribution of the order $D(\xi_j)/Z \sim \Delta_0\kappa$. This, in turn, leads to the enhancement of the value of the order parameter on the chosen site i. These *qualitative* considerations allow one to estimate the position of the conditional distribution average $\Delta_{av}(\xi) = \int d\Delta \times \Delta P(\Delta,\xi)/P(\xi)$ as an appropriate solution to the following system of equations:

$$\Delta_{av} \approx \Delta_{neighb}\left(1 + \lambda \ln \frac{\langle\Delta\rangle}{\Delta_{neighb}}\right), \tag{59}$$

$$\Delta_{neighb} \approx \langle\Delta\rangle + \kappa\Delta_0 \frac{\Delta_{av}}{\sqrt{\Delta_{av}^2 + \xi^2}}. \tag{60}$$

At large values of ξ the solution Δ_{av} approaches the total expectation $\langle\Delta\rangle$, while at $\xi \to 0$ the result behaves as $\Delta_{av} \approx \langle\Delta\rangle + \kappa\Delta_0$, in full agreement to what is observed on Fig. 4. A plot of the full dependence $\Delta_{av}(\xi)$ is presented on Fig. 5 and shows a reasonable agreement with both data obtained from the direct numerical solutions of the self-consistency equations and the curve calculated by appropriate numerical integration of the theoretical expression Eq. (30).

We would like to emphasize, however, that this behavior is subject to revision upon introduction of the Onsager reaction term discussed in Sec. II C. While we expect that for $Z \geqslant Z_1$ this term is of little importance for the distribution function of the order parameter, the profile of the *on-site joint* distribution function $P(\Delta,\xi)$ at $|\xi| \sim \Delta$ can potentially experience noticeable deformations from the described behavior. Indeed, the physical interpretation of the reaction term is to mediate the self-action of the order parameter, that is, the indirect response of a given quantity to its own change through the corresponding responses of the neighboring fields. The latter mechanism is precisely what leads to the described profile of the joint probability function at small values of $|\xi|$. That is why even for sufficiently large values of Z the Onsager reaction term might have a significant effect on the shape of the on-site joint distribution function $P(\Delta,\xi)$ for $|\xi| \sim \Delta$.

It is also worth mentioning that the joint probability distribution $P(\Delta,\xi)$ is of more physical significance than the distribution $P(\Delta)$ of the order parameter alone. Indeed, computation of various physical observables for the given configuration of the order parameter involves values both ξ and Δ for states close to Fermi level, i.e., with $|\xi| \sim \Delta$. As Figs. 4 and 5 suggest, treating fields ξ and Δ as independent would thus result in qualitatively incorrect results. One particular example of this is the spectrum of collective low-energy excitations discussed in Ref. [15]: The inverse Green's function of those modes is sensitive to on-site values of ξ and Δ in equal measures, so computing the average Green's function actually demands the aforementioned joint distribution close to the Fermi surface. Another important question yet to be analyzed is the connection between the field of the order parameter Δ discussed in this paper and experimentally measurable quantities. While the order parameter in weakly disorder superconductors can be probed, e.g., via the single-particle DoS [21], no theory exists to our knowledge of a similar connection in the case of strong disorder with a pseudogap. We believe such a theory will inevitably require the knowledge of joint distribution functions of both ξ and Δ.

G. The effect of weak fluctuations of the coupling amplitudes

In this subsection, we analyze a generalization of our model that allows for the fluctuations of the interaction matrix element between each pair of interacting single-particle states. We model these fluctuations by assigning a random magnitude to the bare matrix element D_{ij} of the interaction between each pair of interacting states on top of its smooth dependence on the energy difference $\xi_i - \xi_j$ of the two states. This corresponds to the following generalization of the self-consistency Eq. (4),

$$\Delta_i = \sum_{j\in\partial i} c_{ij} D(\xi_i - \xi_j) \frac{\Delta_j}{\sqrt{\Delta_j^2 + \xi_j^2}}, \tag{61}$$

where $D(\xi)$ is the energy dependence of the interaction described previously, and c_{ij} are independent random variables distributed according to some distribution $P(c)$. In particular, letting $P(c) = \delta(c-1)$ leads one back to the self-consistency Eq. (4) analyzed earlier. The new Eq. (61) now includes two sources of disorder: the randomness of the single-particle energies ξ_i and the one from the distribution of the coupling matrix elements $D_{ij} = c_{ij}DD(\xi_i - \xi_j)$.

One can conduct the mean-field analysis of Eq. (61) similar to that of Sec. II D. The latter is still valid for sufficiently large number of neighbors, i.e., $\langle c\rangle Z \times 2\nu_0\Delta \gg 1$. One can then assert a spatially uniform order parameter for energies close

to the to Fermi surface and obtain

$$\Delta_R = 2E_0 \exp\left\{-\frac{1}{\lambda_R}\right\}, \quad \lambda_R = \langle c\rangle 2\nu_0 D(0) Z, \tag{62}$$

where λ_R is the new dimensionless Cooper attraction constant, and the value of $E_0 \sim \varepsilon_D$ is still determined by higher energy scales, but with the new value of the mean matrix element.

Our theoretical approach can be generalized to describe the model above, as explained in detail in Sec. G of the SM [26]. In particular, the m function retains its role of the central object in the theory. Here, we only present the proper counterpart of Eqs. (24) and (25) valid for $x \lesssim \varepsilon_D/\Delta_0$:

$$m_1(w) = m_1(0) + \boxed{\langle c^2\rangle}\kappa w\alpha + \boxed{\langle c\rangle}\lambda \int_0^1 dw_1 \sqrt{1-w_1^2}\frac{m_1(w_1,0)-m_1(0,0)}{w_1} + \lambda\int_0^\infty dy_1 \times y_1 \ln\frac{1}{y_1}\int_{\mathbb{R}-i0}\frac{ds}{2\pi}\boxed{\int dcP(c)} \times \boxed{c}\exp\{i\boxed{c}s\kappa w\} \times \exp\{m(s|0,0) - isy_1\}, \tag{63}$$

$$m_2(S|w) = \lambda\boxed{\int dcP(c)}\int_0^1 dw_1 \frac{\exp\{iS\kappa\boxed{c}w_1\} - 1 - iS\kappa\boxed{c}w_1}{w_1^2\sqrt{1-w_1^2}}\left[1 - w_1\left(1-w_1^2\right)\frac{\partial}{\partial w_1}\right] \times \left[\frac{\boxed{c}\kappa w + m_1(w_1)}{\kappa}\right]. \tag{64}$$

In these equations, the boxes highlight the difference brought in by the fluctuations of the matrix element in comparison with Eqs. (24) and (25). Once the solution to these equations is found, expressions Eqs. (30) and (31) for the probability density of the dimensionless order parameter $P_0(y)$ and the joint probability density $P(x, y)$ of on-site values of $x = \xi_i/\Delta_0$ and $y = \Delta_i/\Delta_0$ are applicable without modifications.

1. Generalization to fluctuating number of neighbors Z

We first note that these equations allow one to effortlessly analyze the effect of the fluctuating number of neighbors Z. To this end, one lets $P(c) = p\delta(1-c) + (1-p)\delta(c)$, so each edge is either turned on with probability $p \in [0, 1]$, or turned off with probability $1-p$. As a result, each site has a fluctuating number of neighbors with Poisson distribution characterized by mean value $\langle Z\rangle = pZ$. With such choice of the distribution function $P(c)$, one can explicitly perform all the averages in Eqs. (63) and (64). Remarkably, the outcome *is identical to* the Eqs. (24) and (25) for the case without fluctuations of the number of neighbors upon proper renormalization of the microscopical constants $\lambda, \alpha, Z, \Delta_0, \kappa$, namely, one simply has to replace

$$\lambda \mapsto \lambda_R = p\lambda, \quad \alpha \mapsto \alpha_R = p\alpha \tag{65}$$

and calculate all other low-energy quantities in the theory using these modified values. One particular example of this is the mean-field value of the order parameter Eqs. (62) that now contains precisely λ_R in both the exponent and the prefactor E_0 defined by higher energies. Consequently, the remaining microscopical constants are renormalized as

$$Z_R = pZ, \quad \kappa_R = \frac{\lambda_R}{\Delta_R Z_R}. \tag{66}$$

The derivation of these results is presented in Subsec. G5 of the SM [26]. We once again underscore that such a picture implies absence of any practical significance of the fluctuations of the number of neighbors in our model.

2. Weak fluctuations of the coupling constant λ

A more complicated situation arises, however, if one introduces disorder in the value of c itself. For this calculation, we choose c to be distributed according to a narrow distribution with mean value $\langle c\rangle = 1$, variance $\langle (c-1)^2\rangle = \delta^2$ and exponentially decaying tails. One can then repeat the asymptotic analysis of Sec. III D to extract the influence of the introduced fluctuations of the coupling matrix elements on the extreme value statistics. A detailed exposition is presented in Sec. G of the SM [26], while here we summarize the key results and qualitative conclusions.

In the region of small value of y, that corresponds to a unique saddle point of the form $S = +it$, $t \gg 1$, one can expand the Eq. (63) with respect to small deviations of c from its mean value. Upon estimating the probability Eq. (31) with the help of the resulting asymptotic expression, the double-exponential asymptotic behavior described by Eqs. (46) and (47) remains valid with only a slight modification of the form

$$\zeta(y) \mapsto \zeta(y)\exp\{\delta^2/2\}. \tag{67}$$

However, with finite δ this regime now extends only to a finite lower value of the probability density:

$$P_0(y) \gtrsim \frac{1}{\sqrt{2\pi\lambda\langle y\rangle\kappa\delta^2}}\exp\left\{-\frac{\lambda\langle y\rangle}{\kappa\delta^2}\right\}. \tag{68}$$

This also implies that the double-exponential regime is only present while

$$\delta \lesssim \sqrt{\lambda/\kappa} = \sqrt{Z_{\text{eff}}}. \tag{69}$$

The value of $P_0(y)$ for larger values of δ is described by a different asymptotic behavior with much slower decay in the region of small $y/\langle y\rangle$. It can be interpreted as a change in the type of the dominating optimal fluctuation that delivers the body of the distribution for low values of the order parameter. Indeed, for the case with $\delta = 0$ the only way to render a small value of the order parameter was to have all neighboring values of $|\xi|$ large enough, as explained in Sec. III D. However, sufficiently strong fluctuations of the coupling constant provide a finite probability of a region with a

diminished value of the coupling constant to neighboring sites with relatively small values of ξ. The behavior of the distribution would thus reflect the competition between these two sets of configurations. As a consequence, one expects that in this case the answer will be sensitive to the particular form of the distribution $P(c)$ as well as any local correlations present in the joint distribution of the coupling matrix elements c_{ij} and the on-site energies ξ_i.

The asymptotic behavior of the distribution for large values of the order parameter can also be analyzed within the perturbative expansion of Eq. (63) with respect to the small deviation of c from its mean value. One obtains that each of the multiple saddles point of the integral Eq. (31) for the probability acquire an additional multiplier that can be estimated as

$$P_0^{(n)}(y) \sim P_0^{(n)}(y, \delta = 0) \times \exp\left\{\frac{(z_n\delta)^2}{2}\frac{y - \langle y\rangle}{\kappa}\right\}, \qquad (70)$$

where $z_n = iS_n\kappa$ describes the position of the corresponding saddle point and $P_n(y, \delta = 0)$ stands for the magnitude of the contribution without fluctuations of the matrix element. This result implies that the asymptotic expression Eq. (49) delivered by the main saddle point with $n = 0$ remains *qualitatively* intact up to $\delta \sim 1$, at which point the perturbative expansion with respect to small δ ceases to be applicable. Furthermore, each secondary saddle point acquires an extra multiplier of the form $\exp\{-\frac{(2\pi n\delta)^2}{2}\frac{y-\langle y\rangle}{\kappa}\}$ due to the imaginary part z_n which is close to $2\pi n$. As a result, the oscillations produced by these secondary saddle points are suppressed at $2\pi\delta \sim 1$.

Figure 6 below presents the demonstration of the qualitative picture presented above in the form of both theoretical curves and histograms obtained from direct numerical solution of the modified self-consistency Eq. (61) for several realizations of the disorder. In particular, it clearly illustrates the persistence of both asymptotic trends observed in Sec. III D, while also demonstrating how the secondary maxima are smeared as the value of δ is growing.

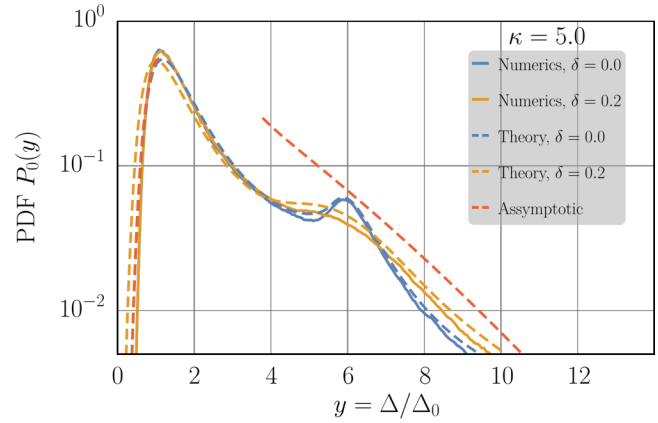

FIG. 6. A log-scale plot for the PDF of the dimensionless order parameter $P(\Delta/\Delta_0)$ for various strengths of the fluctuations of the interaction matrix element $D_{ij} = c_{ij}D(\xi_i - \xi_j)$. The distribution of c is log normal with parameters that ensure $\langle c\rangle = 1$, $\langle(c-1)^2\rangle = \delta^2$. The solid lines represent the smoothened histogram obtained from direct numerical solution of the self-consistency Eq. (61) on three instances of random regular graph of size $N = 2^{17} \approx 1.3 \times 10^5$. The dashed lines use the proper generalization of the weak coupling approximations of Sec. III C to approximate the value of the m function used to compute the integral Eq. (31) for the PDF. Finally, the dashed red line corresponds to approximate analytic expressions for the case without fluctuations of coupling matrix element: Eq. (49) for large values of $y > \langle y\rangle$ and Eqs. (46) and (47) for $y < \langle y\rangle$. The microscopic parameters of the model are $D(\xi) = \text{const}$, $\lambda \approx 0.120$, $Z = 51$, and $\kappa = 5.0$. The mismatch between the theoretical description and the numerical histogram originates from subleading corrections of order $O(\Delta_0/\lambda)$ and $O(\lambda^2)$, see also notes on this under Fig. 2.

IV. DISCUSSION AND CONCLUSIONS

In the present paper, we developed a systematic theory able to describe statistics of superconducting order parameter in strongly disordered pseudogapped superconductors. We have discovered the existence of a wide region of parameters where the usual semiclassical approach to dirty superconductors is not valid but, at the same time, the universal behavior typical for the close proximity to SIT [23] does not take place either. In this wide range of parameters, the shape of the distribution function $P(\Delta)$ is controlled by the single parameter κ defined in Eq. (9). Small κ corresponds to the limit of weak disorder that is typical for usual dirty superconductors. This limit is characterized by narrow Gaussian distribution of the order parameter is observed, see Eq. (43). On the other hand, at $\kappa \gtrsim \lambda$, with λ being the dimensionless Cooper constant, the distribution becomes highly nontrivial. We are able to calculate its explicit form for all values of Δ/Δ_0 in terms of certain special functions, as presented in Sec. III C. The asymptotic behavior of the distribution density $P(\Delta)$ is given by Eqs. (46), (47), and (49) for small and large values of Δ/Δ_0, respectively. These functions do depend on the value of κ; in principle, it opens the possibility to extract the value of κ for specific disordered superconductor via measuring the local distribution $P(\Delta)$ by means of scanning tunneling methods. Our model, however, breaks down in a small vicinity of the SIT described by exponentially large values of $\kappa \gtrsim \exp\{\frac{1}{2\lambda}\} \gg 1$. The phase diagram following from our findings is sketched in Fig. 7.

We emphasize that the very existence of a separate region with a broad range of disorder strengths featuring a nontrivial profile of the distribution function $P(\Delta)$ is related to the smallness of Cooper attraction constant $\lambda \ll 1$. Until recently, the small λ region was not attainable for direct numerical simulations of real 2D and 3D systems due to size restrictions. Advances in this field [35–37] seem to make such a study possible.

The shape of distribution function $P(\Delta)$ was found to differ considerably from the fat-tail distributions obtained previously in Refs. [23,25] by different analytic and numerical methods. Concerning available experimental data, we note, first, that the interpretation of the tunneling conductance dI/dV in terms of the theoretical order parameter is not straightforward in the case of large spatial fluctuations $\Delta(\boldsymbol{r})$. Indeed, in such a case the half width of the gap defined as the energy distance between the peaks in dI/dV is not just given by the order parameter Δ itself, as is the case in the classical superconductor with constant Δ. In fact, the shape of dI/dV is controlled by the local DoS $\nu(E)$ which should be obtained, in principle, via the solution of the generalized

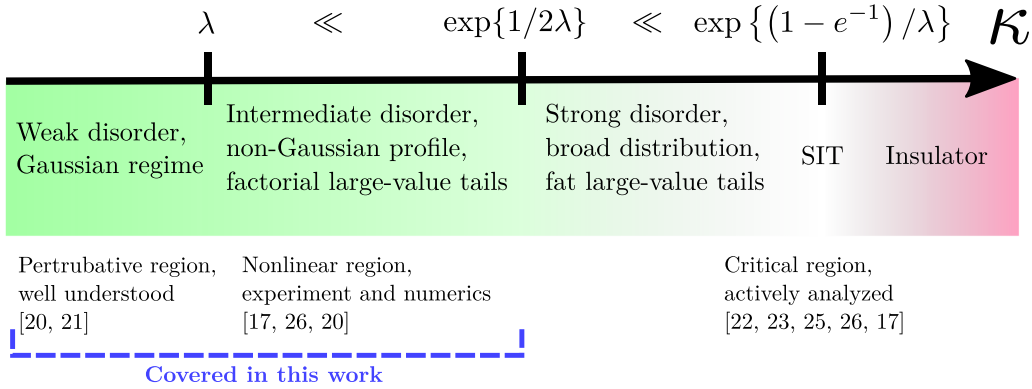

FIG. 7. Qualitative phase diagram describing the behavior of the distribution of the order parameter $P(\Delta)$ in strongly disordered superconductors. The horizontal axis schematically describes the strength of disorder measured by the parameter κ defined in Eq. (9). Various colors indicate the perceived level of inhomogeneity of the superconducting state: the green color corresponds to a well-pronounced superconducting state with nearly uniform value of the order parameter, light-green and white colors represent a manifestly nonuniform superconducting state with strongly non-Gaussian or even critical distributions of the order parameter, and the red color stands for the insulating state of the system with no superconducting order parameter. The blue dashed line highlights the range of parameters available to our theoretical description.

Usadel equation for the local electron Green's function in the background of spatially fluctuating order parameter $\Delta(\boldsymbol{r})$ as well as in presence of a pseudogap. Such a program had never been implemented yet, to our knowledge.

Qualitatively, it seems evident that more direct access to the local values of $\Delta(\boldsymbol{r})$ is provided by the heights R of the coherence peaks in local tunneling conductance $dI/dV(\boldsymbol{r})$. Early experimental data [17] demonstrates substantial change in the distribution of peak heights $\mathcal{P}(R)$ with the increase of disorder, similarly to the effect of increasing our theoretical parameter κ upon the shape of $P_0(\Delta)$, see Fig. 2. Another type of theoretical analysis provided in Ref. [25] predicts an extremely broad distribution of the Tracy-Widom universal shape in terms of the logarithmic variable $R_s = \ln R/\langle R\rangle$; however, their experimental data in Fig. 6 of that paper leaves space for different interpretations as well. A recent study [36] of a strongly disordered 3D superconductor by means of the numerical solution of Bogolyubov-De Gennes equations provides a number of various distribution functions for $P(\Delta)$, which could be analyzed in terms of our theory; for now, we can say that the generic feature—an increase of normalized width of the distribution with disorder—is reproduced there as well.

The model we have studied here is limited in several regards. First, our initial model approximates the matrix element of the Cooper attraction by a constant value that is further endowed with a weak dependence energy difference. However, the actual amplitude of the interaction in each disorder realization is proportional with the overlap of the corresponding wave functions $\int \psi_i^2(\boldsymbol{r})\psi_j^2(\boldsymbol{r})d\boldsymbol{r}$ and thus exhibits direct statistical fluctuations at least of the order of its mean value. In Sec. III G, we have briefly analyzed an extended model that incorporates this effect in the simplest fashion possible. Our analysis indicates that these direct statistical fluctuations do not alter our conclusions about the large-value asymptotic behavior of the distribution of the order parameter, while only removing several unphysical features such as secondary maxima. However, it also follows from our results that even relatively small fluctuations of the interaction matrix element can distort the low-value asymptotic behavior of the distribution of the order parameter. The character of this distortion is generally sensitive to the local structure of the distribution of the matrix elements and requires further analysis.

Second, the energy dependence of the matrix element $D(\omega = |\xi_i - \xi_j|)$ is assumed to be smooth at the relevant energy scale of Debye energy ε_D. It is not necessarily the case for strongly disordered superconductors with the Fermi energy located inside the localized band; the point is that the relevant matrix elements between localized eigenstates contain [27, Sec. 2.2.5] the Mott resonances leading to a singular behavior $D(\omega) \propto |\ln \omega/\delta_L|^{d-1}$. This feature can be incorporated in our approach as long as the overall separation of scales $\Delta \ll \varepsilon_D, E_F$ is maintained.

Third, we have analyzed the mean-field equations for $T = 0$ only. Nonzero temperatures can be included into our formalism simply by multiplying the function $f(\xi_j, \Delta_j|\xi_i)$ defined in Eq. (15) by $\tanh \frac{\sqrt{\Delta_j^2+\xi_j^2}}{2T}$. It will complicate further analysis, but low-T corrections to the obtained results are possible to derive.

The nearest extensions of the developed theory will contain a study of low-energy collective modes in strongly disordered superconductors. The aim is to revisit this subject, considered originally in Ref. [15], with the presently developed understanding about the order parameter distribution. Another important subject is to include the Onsager reaction term in our free-energy functional; it would allow us to consider the region closer to SIT by our methods. Finally, it is of practical importance to establish a reliable connection between the order parameter Δ studied in this paper and experimentally measurable quantities, as none such connections exist to date for strongly disordered superconductors.

ACKNOWLEDGMENTS

We are grateful to Yan Fyodorov, Lev Ioffe, and Igor Poboiko for many useful discussions. A.V.K. is also

grateful to Vladislav P. Serebrennikov for his assistance with the hardware for numerical computations. This research was supported by the Russian Science Foundation Grant No. 20-12-00361.

[1] D. B. Haviland, Y. Liu, and A. M. Goldman, Onset of Superconductivity in the Two-Dimensional Limit, Phys. Rev. Lett. **62**, 2180 (1989).
[2] M. P. A. Fisher, Quantum Phase Transitions in Disordered Two-Dimensional Superconductors, Phys. Rev. Lett. **65**, 923 (1990).
[3] S. L. Sondhi, S. M. Girvin, J. P. Carini, and D. Shahar, Continuous quantum phase transitions, Rev. Mod. Phys. **69**, 315 (1997).
[4] R. Fazio and H. Van Der Zant, Quantum phase transitions and vortex dynamics in superconducting networks, Phys. Rep. **355**, 235 (2001).
[5] V. F. Gantmakher and V. T. Dolgopolov, Superconductor–insulator quantum phase transition, Phys. Usp. **53**, 1 (2010).
[6] B. Sacepe, M. Feigel'man, and T. Klapwijk, Quantum breakdown of superconductivity in low-dimensional materials, Nat. Phys. **16**, 734 (2020).
[7] B. Douçot and L. B. Ioffe, Physical implementation of protected qubits, Rep. Prog. Phys. **75**, 072001 (2012).
[8] P. Brooks, A. Kitaev, and J. Preskill, Protected gates for superconducting qubits, Phys. Rev. A **87**, 052306 (2013).
[9] P. Groszkowski, A. Di Paolo, A. L. Grimsmo, A. Blais, D. I. Schuster, A. A. Houck, and J. Koch, Coherence properties of the 0-π qubit, New J. Phys. **20**, 043053 (2018).
[10] J. E. Mooij and C. J. P. M. Harmans, Phase-slip flux qubits, New J. Phys. **7**, 219 (2005).
[11] J. E. Mooij and Yu. V. Nazarov, Superconducting nanowires as quantum phase-slip junctions, Nat. Phys. **2**, 169 (2006).
[12] M. Tinkham, *Introduction to Superconductivity* (Mac-Graw-Hill Inc., New York, London, Tokyo, 1996).
[13] B. Sacépé, The fate of the superfluid density near the SIT in amorphous superconductors, Bull. Am. Phys. Soc. **66**, L49.00003 (2021).
[14] D. Sherman, U. S. Pracht, B. Gorshunov, S. Poran, J. Jesudasan, M. Chand, P. Raychaudhuri, M. Swanson, N. Trivedi, A. Auerbach, M. Scheffler, A. Frydman, and M. Dressel, The Higgs mode in disordered superconductors close to a quantum phase transition, Nat. Phys. **11**, 188 (2015).
[15] M. V. Feigel'man and L. B. Ioffe, Microwave Properties of Superconductors Close to the Superconductor-Insulator Transition, Phys. Rev. Lett. **120**, 037004 (2018).
[16] B. Sacépé, C. Chapelier, T. I. Baturina, V. M. Vinokur, M. R. Baklanov, and M. Sanquer, Pseudogap in a thin film of a conventional superconductor, Nat. Commun. **1**, 140 (2010).
[17] B. Sacépé, T. Dubouchet, C. Chapelier, M. Sanquer, M. Ovadia, D. Shahar, M. Feigel'man, and L. Ioffe, Localization of preformed cooper pairs in disordered superconductors, Nat. Phys. **7**, 239 (2011).
[18] A. Kamlapure, T. Das, S. C. Ganguli, J. B. Parmar, S. Bhattacharyya, and P. Raychaudhuri, Emergence of nanoscale inhomogeneity in the superconducting state of a homogeneously disordered conventional superconductor, Sci. Rep. **3**, 2979 (2013).
[19] R. Ganguly, I. Roy, A. Banerjee, H. Singh, A. Ghosal, and P. Raychaudhuri, Magnetic field induced emergent inhomogeneity in a superconducting film with weak and homogeneous disorder, Phys. Rev. B **96**, 054509 (2017).
[20] I. Tamir (private communication).
[21] A. I. Larkin and Yu. N. Ovchinnikov, Density of states in inhomogeneous superconductors, Zh. Eksp. Teor. Fiz. **61**, 2147 (1971) [Sov. Phys. JETP **34**, 1144 (1972)].
[22] L. B. Ioffe and M. Mézard, Disorder-Driven Quantum Phase Transitions in Superconductors and Magnets, Phys. Rev. Lett. **105**, 037001 (2010).
[23] M. V. Feigel'man, L. B. Ioffe, and M. Mézard, Superconductor-insulator transition and energy localization, Phys. Rev. B **82**, 184534 (2010).
[24] A. Ghosal, M. Randeria, and N. Trivedi, Inhomogeneous pairing in highly disordered s-wave superconductors, Phys. Rev. B **65**, 014501 (2001).
[25] G. Lemarié, A. Kamlapure, D. Bucheli, L. Benfatto, J. Lorenzana, G. Seibold, S. C. Ganguli, P. Raychaudhuri, and C. Castellani, Universal scaling of the order-parameter distribution in strongly disordered superconductors, Phys. Rev. B **87**, 184509 (2013).
[26] See Supplemental Material at http://link.aps.org/supplemental/10.1103/PhysRevB.104.224505 for technical details of the derivation presented in the main text as well as a detailed discussion of several extensions to the original model aimed at analyzing the robustness of the employed theoretical approach.
[27] M. V. Feigel'man, L. B. Ioffe, V. E. Kravtsov, and E. Cuevas, Fractal superconductivity near localization threshold, Ann. Phys. **325**, 1390 (2010).
[28] M. Ma and P. A. Lee, Localized superconductors, Phys. Rev. B **32**, 5658 (1985).
[29] K. Bouadim, Y. L. Loh, M. Randeria, and N. Trivedi, Single- and two-particle energy gaps across the disorder-driven superconductor-insulator transition, Nat. Phys. **7**, 884 (2011).
[30] B. Bollobás, *Random Graphs*, 2nd ed., Cambridge Studies in Advanced Mathematics, Vol. 73 (Cambridge University Press, Cambridge, 2001).
[31] M. Mézard and G. Parisi, The Bethe lattice spin glass revisited, Eur. Phys. J. B **20**, 217 (2001).
[32] M. Mézard and G. Parisi, The cavity method at zero temperature, J. Stat. Phys. **111**, 1 (2003).
[33] B. D. McKay, The expected eigenvalue distribution of a large regular graph, Linear Algebra Appl. **40**, 203 (1981).
[34] A. V. Khvalyuk, Numerical routine for solving the integral equations on the cumulant generating function of the order parameter, 2021, GitLab repository: https://gitlab.com/AnwardoX/OP-distribution-numerics.
[35] M. Stosiek, B. Lang, and F. Evers, Self-consistent-field ensembles of disordered Hamiltonians: Efficient solver and application to superconducting films, Phys. Rev. B **101**, 144503 (2020).
[36] B. Fan and A. M. García-García, Superconductivity at the three-dimensional Anderson metal-insulator transition, Phys. Rev. B **102**, 184507 (2020).
[37] A. Datta, A. Banerjee, N. Trivedi, and A. Ghosal, New paradigm for a disordered superconductor in a magnetic field, arXiv:2101.00220.